



**CHALMERS**  
UNIVERSITY OF TECHNOLOGY

---



# **Autonomous WaveRunner Follow the Leader**

Development of an autonomous path following system for a personal watercraft

Bachelor's thesis in Electrical Engineering

Erik Ingemarsson  
Fredrik Kerstis  
Petter Lindesson  
Martin Löfgren  
Hakim Male  
Felix Millqvist





## Autonomous WaveRunner | Follow the Leader

Bachelor Thesis Project EENX15-19-02  
Department of Electrical Engineering  
Chalmers University of Technology  
412 96 Gothenburg, Sweden  
June 5, 2019

### Authors:

Erik Ingemarsson  
inerik@student.chalmers.se

Fredrik Kerstis  
kerstis@student.chalmers.se

Petter Lindesson  
petlinde@student.chalmers.se

Martin Löfgren  
marlofg@student.chalmers.se

Hakim Male  
hakimm@student.chalmers.se

Felix Millqvist  
felixmi@student.chalmers.se

### Examiner:

Petter Falkman  
petter.falkman@chalmers.se

### Supervisor:

Torsten Wik  
tw@chalmers.se

### SSRS Representative:

Fredrik Falkman  
fredrik.falkman@ssrs.se

**Autonomous WaveRunner** constitutes a long-standing collaboration between the Swedish Sea Rescue Society (SSRS) and Chalmers University of Technology, founding a series of coherent Bachelor and Master thesis projects regarding the conversion of a personal watercraft for implementation of autonomous abilities.

**Keywords** Autonomous Watercraft, Watercraft Control, Watercraft Modelling, Path Following, Sea Rescue, Naval Automation, RescueRunner.



## Abstract

A customized personal watercraft is commonly used by the Swedish Sea Rescue Society during rescuing operations. Transportation to and from accident sites have proved problematic, creating the need for an alternative transportation method. The proposed solution is that the vessel autonomously follows a lead craft during transportation.

This report presents the hardware and software implementation of an autonomous system, disregarding the implementation of a signal actuator system, due to it being constructed by a parallel project. To obtain its functionality, two positional sensors utilizing GPS technology, a radio communication link, and an small computer running a PID control system were used.

A navigational algorithm was constructed to calculate a desired change of heading and current distance to the lead craft, which were used as reference values for the controllers. This algorithm was designed by the use of a look ahead method.

Data captured from the constructed simulation model indicates that the system is functional. Through tuning of control parameters, the system was able to follow a sampled test path in an acceptable manner. Improvements were achieved when modeling the steering controller to also use throttle as an input. This improved the system's ability of handling varying velocities.

The system is ready for field testing where further tuning of control parameters can be done to compensate for deficiencies in the simulation model. These tests are to be performed after report hand in deadline due to time constrains.

## Acknowledgements

We would like to thank our thesis advisor, assistant professor Torsten Wik, our guardian examiner, assistant professor Petter Falkman, and assistant supervisor Rikard Karlsson, at the Department of Electrical Engineering at Chalmers. We also want to express our gratitude to our main contact person at the Swedish Sea Rescue Society, Fredrik Falkman.

# Table of Contents

<b>1</b>	<b>Introduction</b>	<b>1</b>
1.1	Background . . . . .	1
1.2	Purpose . . . . .	2
1.3	Delimitations . . . . .	2
1.4	Previous Studies . . . . .	3
1.5	Report Structure . . . . .	3
<b>2</b>	<b>System Design</b>	<b>5</b>
2.1	Method . . . . .	5
2.2	Specification of Requirements . . . . .	5
2.3	Specification of Functionality . . . . .	6
2.4	System Configuration . . . . .	7
2.4.1	Sensors & Input Aata . . . . .	7
2.4.2	Communication . . . . .	9
2.4.3	Computing Devices . . . . .	10
2.5	Alternative system configurations . . . . .	10
2.6	Hardware Installation & Connections . . . . .	12
2.6.1	WaveRunner Hardware System . . . . .	12
2.6.2	Lead Craft Hardware System . . . . .	13
2.7	Communication protocols . . . . .	14
<b>3</b>	<b>Navigation</b>	<b>15</b>
3.1	Method . . . . .	15
3.2	Map Projection . . . . .	15
3.3	Path Generation . . . . .	15
3.4	Path Following . . . . .	16
3.4.1	Distance from WR to LC . . . . .	16
3.4.2	Direction of the WR . . . . .	17
3.5	Output . . . . .	20
<b>4</b>	<b>Model</b>	<b>21</b>
4.1	Method . . . . .	21
4.2	Coordinate Systems . . . . .	21
4.3	Equations of Motion . . . . .	22
4.3.1	General Equation of Resistance . . . . .	23

4.3.2	General Equation of Thrust . . . . .	23
4.3.3	Equation of Surge Motion . . . . .	24
4.3.4	Equation of Sway Motion . . . . .	25
4.3.5	Equation of Yaw Motion . . . . .	25
4.3.6	State Variables Subsystem . . . . .	25
4.4	Verifying Model . . . . .	26
4.4.1	Scaling of Forwards Momentum . . . . .	27
4.4.2	Scaling of Rotational Resistance and Thrust . . . . .	28
4.4.3	Scaling of Lateral Resistance and Thrust . . . . .	28
<b>5</b>	<b>Control System</b>	<b>29</b>
5.1	Method . . . . .	29
5.2	Overall Control System . . . . .	29
5.3	Throttle Control . . . . .	30
5.4	Steering Control . . . . .	30
5.5	Implementation . . . . .	31
5.6	Simulation . . . . .	31
<b>6</b>	<b>Discussion &amp; Conclusion</b>	<b>41</b>
6.1	Discussion . . . . .	41
6.2	Future Development . . . . .	42
6.3	Conclusions . . . . .	44
<b>A</b>	<b>Git Repository Structure</b>	<b>47</b>

## List of Figures

1	Overview of the system's functional specification. . . . .	6
2	Overview of the final system configuration. . . . .	7
3	Specification of ship motions in three dimensions. . . . .	8
4	GNSS units. . . . .	9
5	Holybro Telemetry Radio V3. . . . .	9
6	Computing devices. . . . .	10
7	Hardware connections overview. . . . .	11
8	Overview image of hardware system installed within the WR . . . . .	12
9	Schematic overview of the computer box in the WR . . . . .	13
10	Schematic overview of the portable box on the LC. . . . .	14
11	Distance to LC illustration. . . . .	17
12	Perpendicular distance between the WR and the path. . . . .	17
13	Direction calculation illustration. . . . .	20
14	Axes local to the WaveRunner. . . . .	21
15	Simulink model of the WaveRunner. . . . .	22
16	Simulink subsystem for thrust from a jet. . . . .	24
17	WR angle and Nozzle angle. . . . .	24
18	Simulink subsystem for surge motion. . . . .	25
19	Simulink subsystem for kinematic parameters. . . . .	26
20	Plot for acceleration, showing test and simulation data. . . . .	27
21	Plot for coasting stop, showing test and simulation data. . . . .	27
22	Test and simulation data from steering test . . . . .	28
23	Throtte control system. . . . .	30
24	Steering control system. . . . .	31
25	Simulation set up in Simulink. . . . .	32
26	Throtte control system. . . . .	33
27	Steering control system. . . . .	33
28	Thrust from the nozzle and its components. . . . .	34
29	Simulation run using original velocity. . . . .	35
30	Simulation run with two times the original velocity. . . . .	36
31	Simulation run with two thirds of the original velocity. . . . .	37
32	Simulation after corrections, run using original velocity. . . . .	38
33	Simulation after corrections, run with twice the original velocity. . . . .	39
34	Simulation after corrections, run with two thirds of the original velocity. . . . .	40

## List of Tables

1	Table of system requirements. . . . .	6
2	Variables used in the section. . . . .	18
3	The degrees of freedom used in the modeling of the WR. . . . .	22
4	Constants and their values used in the modelling of the WR. . . . .	23
5	Parameters tuned to test data. . . . .	26
6	The control parameters for simulation used in Figure 29, 30 & 31. . . . .	32
7	The control parameters used in Figure 32, 33 & 34. . . . .	34

# Glossary of Technical Terms

## Abbreviations

## Meaning

### General

SSRS	Swedish Sea Rescue Society
DbW	Drive-by-Wire
WP	Way Point
DoF	Degrees of Freedom
UTM	Universal Transverse Mercator

### Hard- and Software

IMU	Inertia Measurement Unit
GPS	Global Positioning System
GNSS	Global Navigation Satellite Systems
WGS	World Geodetic System
UART	Universal Asynchronous Receiver Transmitter
SPI	Serial Peripheral Interface
<i>I<sup>2</sup>C</i>	Inter-Integrated Circuit
CAN	Controller Area Network
MCU	Micro Controller Unit

### Vessels

WR	WaveRunner
RR	RescueRunner
LC	Lead Craft



# 1 Introduction

This report constitutes the final result of a bachelor thesis project, *WaveRunner - Follow the Leader* (EENX15-19-02), conducted at the Department of Electrical Engineering at Chalmers University of Technology in Gothenburg, Sweden. The thesis work constitutes a part of a larger project conducted in collaboration with the Swedish Sea Rescue Society (SSRS), concerning one of their smaller rescuing vessels called the RescueRunner (RR), a personal watercraft specifically designed for the purpose of sea rescue operations. The aim of the *Follow the Leader* project, concerned within this report, is to design and implement a self-regulating navigation system, providing the vessel with the ability to navigate autonomously along a path provided by a separate lead craft (LC).

The thesis project is conducted in parallel with, but directly related to, a separate thesis work, *WaveRunner - Drive-by-Wire* (EENX15-19-01), covering the implementation of an actuator system enabling the watercraft to be controlled using electronic signals. The development of the Follow the leader project relies on the results generated in this parallel project, regarding several different functionalities of the watercraft system. The entire system generated by the Follow the Leader project is adapted for future expansion and compatibility with further development. Generated programs and functions are constructed on a modular basis, intended to simplify the work of further expansion or development of the integrated system constituents.

## 1.1 Background

The Swedish Sea Rescue Society (SSRS) is a non-governmental organization which, since its foundation in 1907, has been responsible for a vast majority of the emergency sea rescues executed along the Swedish coast. The organization currently engages a total of 2,300 volunteer life-savers providing a continuous 24 hour stand-by, with the possibility to dispatch rescue personnel within 15 minutes after the onset of any alarm, dispatching from any of their 71 bases distributed along the Swedish coastline and larger lakes [1].

During rescue missions, SSRS utilizes a number of rescue vessels of various capacity, depending on local availability and the requirements of each specific rescue mission. In general, larger vessels provide the advantage of easier handling at rough seas, easier long distance transportation, whereas smaller vessels instead provide a higher level of agility and mobility, making them well suited at rescue sites with confined accessibility. In order to provide this high maneuverability, the RR was employed. Due to its favourable properties, the RR is currently one of the most popular types of smaller vessels utilized by the SSRS. It's design is based on a personal watercraft (PWC), providing a lightweight vessel with a low freeboard in combination with a high level of maneuverability, thus well suited for mobility demanding rescue missions [2].

Yamaha WaveRunner is a PWC series manufactured by Yamaha, providing a wide range of models in various levels of performance. During the execution of this project, a PWC of the model Yamaha VXCruiser is considered, henceforth referred to as the WaveRunner (WR). The characteristics of this vessel are considered similar to the ones of the RR used by the SSRS and thus, the results of the project are assumed applicable to the RR as well.

One major disadvantage with smaller vessels, such as the RR or the WR, is that they tend to wear out the driver while travelling longer distances. Because SSRS intends to frequently use the RR, this disadvantage may pose a substantial issue, since resources at rescue sites

stand the risk of being wasted during transport, that may be crucial in the important work following when reaching the actual rescue site. Currently, most of SSRS's bigger vessels are not capable of carrying or towing one of their smaller vessel due to their size and weight, as well as the substantial risk of causing material damage. Altogether, these factors tend to complicate usage of smaller rescue vessels during some rescue missions, and may in many cases prevent the rescuing personnel from operating them at all [2].

The challenges of transporting the smaller rescuing vessels may cause unnecessary strain on the rescuing personnel or prevent the tool from being used at all. The implementation of an autonomous navigation system would have the potential of enabling the SSRS to easily bring their smaller, agile rescue vessels to the rescue site, without standing the risk of causing unnecessary burden for the rescue personnel through the less relevant subtask of taking the vessel to the site [2].

## 1.2 Purpose

The purpose of the project is to construct a navigational system enabling a personal watercraft to autonomously follow a lead craft. This involves the derivation of an algorithm for following the lead craft and the implementation of a driving control system, resulting in a complete hardware and software system prototype, adapted for future development and expansion.

## 1.3 Delimitations

To further define the project's scope, a set of delimitations were specified. These are presented below with accompanying motivations.

**Environmental Conditions:** in order to create a system that is suited for all weather it would demand a lot of resources for performance, implementation and simulation to work. Because of this a stable basic model with the vital and necessary attributes was made that is not suited for strong winds and high tides.

**Obstacle Evasion:** The system does not take obstacle avoidance into consideration. This delimitation was made due to the fact that, provided a well functioning path following algorithm and, an empty and open sea, no obstacles should exist between the two vessels, hence rendering an obstacle evasion system unnecessary. Furthermore, additional sensors would need to be added causing the system to become more complex. During the whole project the WR will always be piloted by a test person who could intervene if an unexpected object would appear.

**Drive-by-Wire System Implementation:** Because of the parallel project the implementation and trial phase of this project presumed a fully functioning Drive-by-wire system where all mechanical actuators are controllable through electrical signals. Instead this thesis has focused on processing positional data and producing a navigational system.

**Control System Extrema:** The control system is not expected to handle extrema. This includes harsh maneuvers from the LC, WR start and stop actions and changes in

water current conditions. Instead the initial main goal is to follow the LC when practicing a reasonably normal behavior, which should exclude such extrema.

**Hardware System:** Several components were selected by the institute to secure potential of further developments. Hence, parts of the system's hardware were not evaluated correctly and no alternative solutions were drafted. Furthermore, all parts of the system were evaluated on the basis on how they could be utilized for further development.

## 1.4 Previous Studies

Several systems for Autonomous surface vessels have been built. For instance, Massachusetts Institute of Technology has produced an autonomous system called ACES [3], which was later renamed AutoCat [4]. This vessel utilizes a Proportional and Derivative-controller in order execute waypoint based path following. However, both systems focused more on the design of the hull and the physical attributes of the vessel.

Other projects concluded that using only key navigational equipment, such as a GPS and a compass, and basic control laws, a robotic marine vehicle could be built [5, 6].

At Chalmers University of Technology five similar projects have been carried out, spanning a period of five years at both bachelors and masters level. The main theme was to automate a smaller rescue vessel. Two bachelor theses were performed in order to robotize the controls of a vessel through different methodologies [7, 8]. Another bachelor thesis was carried out to produce both the hardware and the software needed for remote control and autonomous drive of a rescue vessel. The remote control system was successfully implemented, however, the system for autonomous drive was not [9]. Several ideas from this bachelor thesis will be regarded when choosing components, while the solutions for autonomous drive will not be considered in depth due to it not working.

Two master theses proved, both in theory and in practise, the possibility for an autonomous system to handle the navigation of the vessel. The most recent one focused on building a sensor fusion algorithm based on a Kalman filter for their GPS and IMU units, and concluded that the task posed by the *Follow Me* project is achievable [8]. The other master thesis utilized two PID-controllers, one for gas and one for heading alterations, to navigate between way points [10]. However, the way point based navigation system caused the PWC to sometimes perform with unwanted characteristics, this project will therefore implement an alternative solution.

## 1.5 Report Structure

The report is aimed to be structured in such a way that the results are presented in order of their internal contextuality. It is thus not intended to mirror the chronological order through which the project was carried out, but rather in the logical order of which each specific part of the project is connected to and dependant upon the others.

The content of the report is structured in sections in accordance with the description below.

**2. System Design** presents the process of hardware component selection required within the system to ensure the inclusion of capabilities required to fulfill the project goals. This includes a specification of each of the key components within the final system design.

3. **Navigation** introduces the algorithms used to navigate the WR, ensuring that it follows the LC. Descriptions regarding the internal functionality and technical background of each algorithm is presented.
  4. **Model** explains the derivation of a mathematical model to mimic the dynamical behaviour of the WR when controlled. The aim of this model is to work as a baseline for both the construction and testing of the control system.
  5. **Control System** describes the construction and functional parameters of a control system and its internal subsystems, and presents the methods of calculation of initial control parameter values. The testing of the system in the computerized simulation model described in the section before, and subsequent adjustments of parameters within the control system are also covered.
  6. **Discussion & Conclusion** presents an evaluation of the achieved project results presented in the previous sections above, and discusses the results and conclusions made.
- A. Git Repository Structure** describes the overview of the public GitHub repository containing all code necessary for project execution.

The project and its results consist of a number of separate segments, many of which are achieved using a various range of methods concerning implementation or execution. Therefore, the descriptions of applied methods are not accumulated within one specific section in the project introduction, but distributed across the different sections concerning each particular implementation and result.

## 2 System Design

The main purpose of this section concerns the design of a hardware system which can achieve the functionality specified in Section 1.2. The first parts covers the determination and evaluation of functional and constructional parameters, required for the design of the hardware system. Thereafter, the selected system configuration, fulfilling the stated requirements on the system, and each of its included components, are presented (see Section 2.4). A brief summary of a number of deselected alternative implementations, system technologies and key components, is provided in Section 2.5, along with motivations as to why they were deselected.

### 2.1 Method

The selection of the system layout and its components was carried out on the basis of a number of conventional product development methods. These factors are combined with external project requirements, regarding subjects such as capacity and technology selection, in order to form a complete set of system requirements. Several parts of the construction phase were also affected by a number of project delimitations, regarding subjects such as disturbance caused by environmental factors (see Section 1.3).

The requirements on the complete system were accumulated through studies of the situational and environmental prerequisites by which the system was intended to function. The performance requirements regarding measurement data were estimated on the basis of previous implementations and performance assessments regarding the proposed control system [7].

The selection of components and system technologies was carried out on the basis of the constructional guidelines provided by the specification of requirements and functional specification. This part of the system construction was mainly conducted through dialogue with the project supervisors and representatives for SSRS, generating and evaluating several different technologies and ideas.

### 2.2 Specification of Requirements

The system configuration process was to be determined through the stipulation of a number of essential requirements covering the complete functionality and performance of the system. The different criteria gathered through these studies, their preferred and/or required value or range are defined in Table 1.

The requirement column in Table 1 presents the estimated minimum functionality deemed as necessary for the system to function, and thus required to be fulfilled within the subsequent studies of system configuration and implementation. The preference column aims to specify the range or value of the system criteria that is estimated as eligible for a high-performance system, but not necessarily required in order to acquire basic system functionality. System configurations fulfilling these target values are considered.

Note that in some cases, only one of these values have been defined. If the specified criteria is started as necessary for the system to function, the preference value is left unspecified.

Table 1: Table of system requirements.

Criteria	Requirement	Preference
Relative positioning of LC and WR	$< 4\text{m}$	$< 1\text{m}$
Direction measurement of the WR	$< 5^\circ$	$< 1^\circ$
Update frequency of the lead craft's position	$\geq 2\text{Hz}$	$\geq 10\text{Hz}$
System output through CAN	Required	-
Compatibility for future development	Required	-
Water & dirt resistance	IP67	IP68
Vibration resistance	No	Yes
Weather support	No rain and no wind	Any weather
Communication range between WR & LC	$\geq 100\text{m}$	$\geq 1000\text{m}$

### 2.3 Specification of Functionality

In accordance with the main purpose of the system, as well as the attributes stated within the system specification (see Section 2.2), the properties of the system can be divided into a network of required subtasks, with internal and external connections. These subtasks and connections are necessary for the complete system solution, ensuring the required functionality. The functional overview of the system (see Figure 1) serves as a tool for the construction of the detailed system layout, as well as the selection of components.

The two vessels' relative positioning is required in order to create a frame of reference for the navigational systems. While not necessary for the LC, the WR's directional data and current velocity were needed to verify its current heading in order to be able to control it.

The obtained parameter data was required to be logged, thereafter functioning as reference data for calculation of changes to the WR's current heading and velocity. This subsystem, residing over heading and velocity changes, should utilize the logged data and the feedback signals to calculate adequate control signals for the throttle and steering of the WR, which are then to be provided as control signals to the DBW system. These are then provided with an interface, bridging the system to the steering actuators by two separate signals, one for the throttle and one for the nozzle angle, which are communicated through a CAN bus.

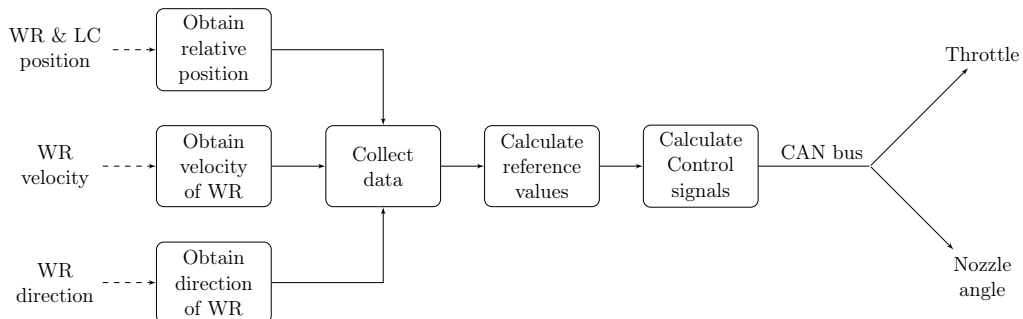


Figure 1: Overview of the system's functional specification. Dashed lines symbolize data acquisition, and arrows symbolize the direction of data flow.

## 2.4 System Configuration

The selection of system technologies and components were based on several factors regarding functional requirements and reliability within the specific areas of intended use. Requirements listed in Section 2.2 were evaluated with documented experiences from previous implementations of the technology in similar conditions, obtained from project reports criteria, as well as further guidelines provided externally for the project. An overview of the final system configuration is presented in Figure 2.

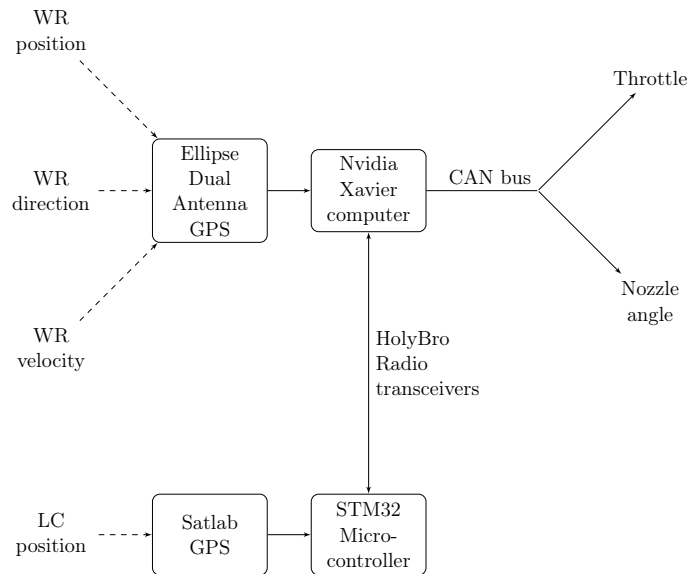


Figure 2: Overview of the final system configuration. Dashed lines symbolize data acquisition, and arrows indicate the direction of data flow.

Worth noting in this configuration is that, instead of acquiring the relative positioning of the two vessels, as illustrated in Figure 1, absolute position data is acquired for both vessels. The relative positioning is then to be calculated within the internal computer system.

A presentation of each specific component in the system layout is provided in the sections below. The specifications and capability of each device has been retrieved from datasheets provided by the manufacturers or from their respective websites. The actual performance of each device at the conditions intended for this specific system may differ to a certain degree from those in the specified references.

### 2.4.1 Sensors & Input Aata

As stated in Section 2.4, absolute positioning of the two vessels was obtain instead of the relative positioning. This caused the need for two different sensor units for the WR and LC respectively. The sensor units both apply GPS technology to obtain positional data with fair accuracy, and feature an optional use of Real Time Kinetic (RTK, a system using fixed antennas sending correctional data via GSM to improve accuracy) GNSS positioning, providing a highly increased measurement precision with a deviation of only a few centimeters. In addition, the two units are each equipped with a pair of dual antennas, enabling

them to also provide a highly accurate heading measurement, with a measurement error of less than  $0.5^\circ$ .

The use of GPS technology is evaluated as the most trustworthy technology for the purpose of the project, whereas the rough conditions of the environment make most forms of relative positioning technology, such as vision cameras or radar, relatively hard to use. The absolute positioning enables the system to gather a series of data points along the path of the LC without requiring an extensive amount of calculations and data processing.

**Ellipse2-D RTK INS** (see Figure 4) is a high-precision GPS receiver intended to function as the main measurement unit on the WR. The Ellipse2-D is equipped with Dual Antennas, providing precise measurement data regarding both position and direction of the vessel. Using the basic GPS positioning system, a position accuracy of approximately 1.2 m is achieved. By activating the optional, integrated RTK GNSS, the accuracy can be enhanced drastically, reaching deviation levels less than 2 cm, according to the specifications. Using a baseline, i.e. distance between antennas, longer than 1 m, the Dual Antennas provide the system with a heading measurement accuracy of at least  $0.2^\circ$  [11].

The unit also features an integrated Inertial Measurement Unit (IMU) which is mainly intended to be available for use in future development projects. The IMU features 3 axis gyroscopes, accelerometers and magnetometers. This enables the system to obtain a complete set of motion data regarding the vessel, in three dimensions. This covers both longitudinal and rotational movement along any axis (see Figure 3). These measurements are specified to reach accuracy levels of approximately  $0.1^\circ$  for the pitch and roll motions, and 5 cm (5 %) heave accuracy, handling wave periods up to 15 seconds [11].

The GPS and motion data is enhanced in real time through internal Extended Kalman filters, lowering the risk of signal deviation caused by GNSS outtages, from e.g. passing under a bridge or environmental disturbances. The unit is adapted for use in harsh environments, compensating for noise caused by vibration through use of internal FIR filtering accelerometers and low noise gyroscopes.

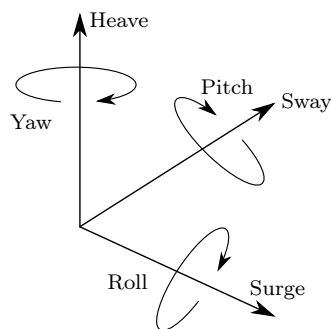


Figure 3: Specification of ship motions in three dimensions.

Note that IMU measurements remain unused throughout this project. A unit covering these extended measurements was selected for inclusion in the system, with the purpose of securing accessibility of this data for future projects.



(a) Ellipse2-D RTK INS.

(b) Satlab UAV/RTK.

Figure 4: GNSS units.

**Satlab UAV/RTK** (see Figure 4b) is a high-precision GPS receiver designed for multi-purpose use especially in unmanned aerial vehicle applications. This device serves as the main measurement unit on the LC. The unit was, equally to the GPS unit on the WR, equipped with Dual Antennas, thus providing both position and direction measurements (usable in future projects) for the vessel.

The basic GPS positioning measurements are specified to attain accuracy levels of approximately 1.5 m. Activation of the featured RTK GNSS functionality results in an increased accuracy to a deviation less than 1 cm.

#### 2.4.2 Communication

In order for the WR to access the relative positioning the LC needs to communicate its positioning to the WR's main computing device. Other solutions, e.g. one utilizing camera and radar instead, would not need communication between the two vessels since the WR could gather the relative positioning from its on-board sensors. To achieve this communication a radio transceiver was used, since it proved to be successful in a previous master work [8]. The transceiver used in this application however, uses a different radio band in order to obtain a greater effective range.



Figure 5: Holybro Telemetry Radio V3.

**Holybro Telemetry Radio V3** (see Figure 5) is a transceiver unit with an open source firmware, making it easy to configure. The unit transmits over the 433 MHz band and offers a range of communication up to 1000 m. These attributes made it suitable for this project.

### 2.4.3 Computing Devices

Both the WR and the LC need computing devices to perform their tasks. For the LC, a less performant device is sufficient as its job is mainly to transform data from the GPS and transmit these to the WR. For the WR, higher performance is needed, mainly for future expansions involving computer vision and other demanding tasks.

**Jetson AGX Xavier** (see Figure 6a) is a high-performance, embedded System-on-module manufactured by Nvidia, used in the WR. The unit features several interfaces relevant to the current and future development of the project, including but not limited to CAN, UART and USB. It has an 8 core 64 bit ARM processor, a 512 core GPU and 16 GB RAM.

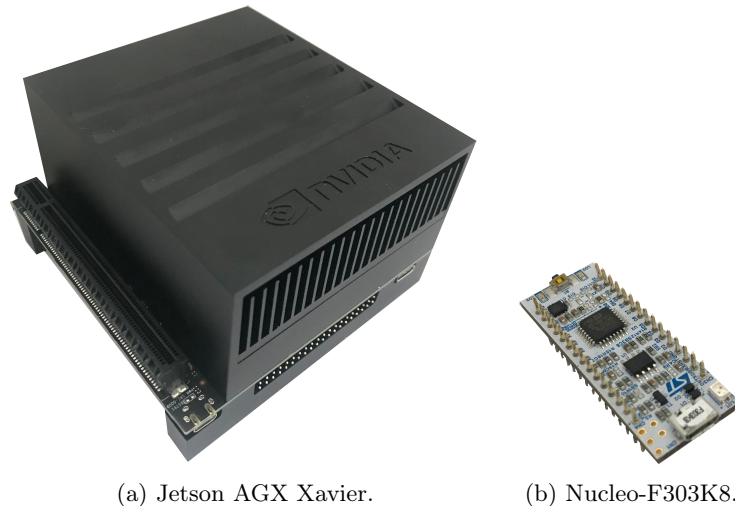


Figure 6: Computing devices.

**Nucleo-F303K8** (see Figure 6b) is a 32-bit, ARM-based microcontroller. It was selected for use on the LC due to its small size, versatility as well as its high capability to perform complex tasks at relatively high speeds consistently and effectively.

## 2.5 Alternative system configurations

In addition to the final system design and the included components presented above, a number of alternative system configurations were considered. The investigation of these alternative systems was limited, due to guidelines and external requirements provided for the project, and was mainly performed to ensure system capacity and abilities. A brief summary presenting the considered, alternative system configurations and technologies is provided in this section.

A few solutions using cameras and radars in order to collect positional data were evaluated. This technology would include cameras or radar mounted on the WR to keep continuous track of the relative position of the LC, which could potentially enable it to follow the leader without the requirement of further installations or adjustments of the LC. Technology as such could also make the system able to detect obstacles, possibly enabling navigation in crowded areas such as harbors.

These sensors would likely require to be mounted high up on the WR and possibly a system for stabilizing the detection unit to ensure that the system does not lose sight of the lead vessel in case of heavy pitch. A camera is also prone to be blinded due to the reflective nature of water, and would also be sensitive to darkness and bad weather, such as fog, heavy rain, etc. These systems would also be limited by the field of view of the detection units, introducing a risk of completely losing the ability to specify its current relative position and direction.

The wireless communication between the LC and the main control unit on the WR would be possible to establish through several different technologies. The 433 MHz radio communication devices selected in this project would be possible to be replaced using e.g. Bluetooth, WiFi or through mobile communication systems such as GSM, 3G or 4G. WiFi connection was implemented in one of the previous bachelor thesis projects in a similar system [10], in which the technology was there found to be as unreliable and unstable. Both WiFi and Bluetooth communication lines are highly dependent on short communication distances, which may be problematic for the project implementation as well as compatibility for further development. Mobile communication systems, in turn, are able to communicate across long distances, and provide a high level of development compatibility. This type of communication is considered more expensive, and may stand risk of connection loss in the type of environment that the system is intended to function.

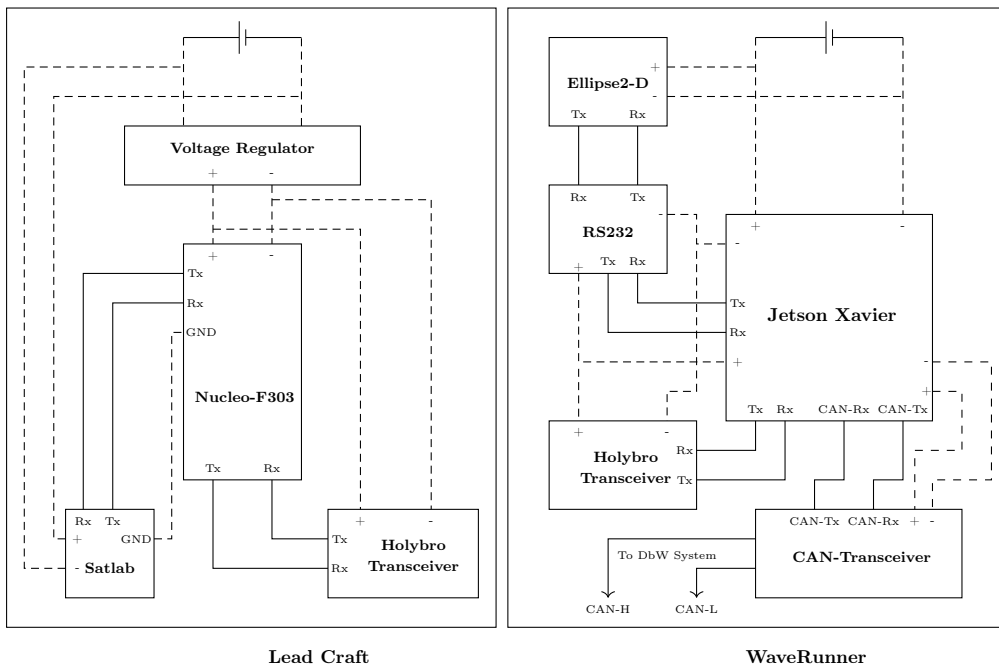


Figure 7: Hardware connections overview.

## 2.6 Hardware Installation & Connections

The purpose of this section is to provide a description of the hardware installations performed in order to achieve a system in accordance to the configuration (see Section 2.4). This system is divided into two physically separate units; one intended for the LC and one for the WR. The physical properties of these two units and their installation are presented in the two sections below. Connection diagrams are provided in Figure 7.

### 2.6.1 WaveRunner Hardware System

The hardware system of the WR was designed for permanent installation within the body of the vessel, although this prototype system was still eligible to maintain some aspects of variability and removability for ensuing projects. An overview image of the system components installed within the WR is provided in Figure 8.

The system is centered around a waterproof (IP68-classed) aluminum box mounted in the bow storage compartment of the WR, containing the main devices; the Nvidia Xavier computer, a HolyBro radio transceiver, a CAN transceiver board and a RS232 to TTL conversion board. A schematic illustration of the box is provided in Figure 9. In order to counteract the heat development within the box, the heatsink of the computer board was connected directly to the aluminum casing of the box using a thermal compound.

The box is equipped with four sockets (see Figure 9). The short edge of the box is equipped with two 4 pin connectors, the first one used for power supply of and serial communication with the Ellipse GPS, and the other one containing a two pin CAN communication interface and power input for the entire system. The long edge of the box is equipped with a coaxial antenna connection for the HolyBro telemetry transceiver antenna, and an ethernet port for optional, external access to the Xavier computer board.

The Ellipse GPS and its antennas are also mounted in the body of the WR, placed in accordance with the illustration in Figure 8. The Ellipse GPS is mounted in the bow storage compartment of the WR, below the computer box, and connected to one of the 4 pin connector of the box for power and serial communication. The Ellipse is connected to a primary antenna mounted on the inside of the lid of the bow compartment, and a secondary antenna mounted on the inside of the body panels in the starboard aft of the WR, accessible through removal of the backseat.

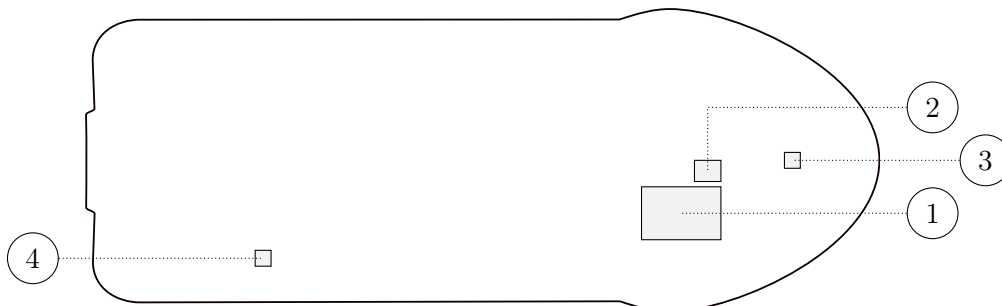


Figure 8: Overview image of hardware system installed within the WR. 1: Computing box, 2: Ellipse GPS, 3: Front antenna, 4: Rear antenna.

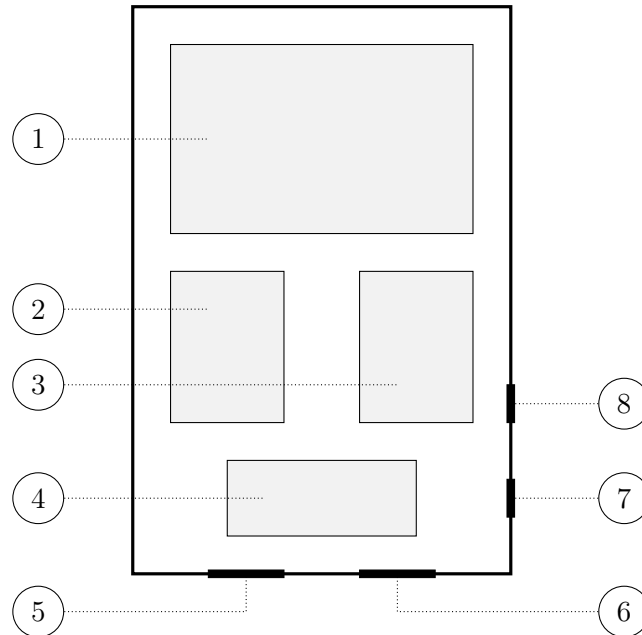


Figure 9: Schematic overview of the computer box in the WR. 1: Jetson AGX Xavier, 2: CAN transceiver, 3: RS232-TTL converter, 4: Holy Bro Radio transceiver, 5: 4 pin connector for GPS communication and power supply, 6: 4 pin connector for CAN and power supply, 7: Coaxial connector for radio antenna, 8: Ethernet port for interfacing the Jetson AGX Xavier.

### 2.6.2 Lead Craft Hardware System

A portable, waterproof (IP68-classed) plastic box was used as enclosure for the LC hardware components. A total of six components were mounted inside; the STM microcontroller, the Satlab GPS, a HolyBro radio transceiver, a lithium polymer battery, a voltage regulating circuit, and a Wi-Fi board. An overview illustration of the box and its internal components is provided in Figure 10.

The lithium polymer battery provides the system with 11.1 V of voltage, run through a voltage regulator. The regulator delivers the full 11.1 V to the Satlab GPS, while simultaneously providing the microcontroller, radio telemetry, and Wi-Fi board with a transformed voltage at 5 V each.

The microcontroller was used for two main purposes, firstly to configure the Satlab GPS and secondly to format the GPS output data to be transmitted via the HolyBro transceiver to the WR.

The NodeMCU Wi-Fi board has been added to the system solely for the purpose of simplifying the testing and tuning of the system. For this purpose, a Hypertext Markup Language (HTML) based graphical user interface was designed, available through the Wi-Fi hotspot provided by the component. Through this wireless interface, accessible through a web browser, control system parameters were made available for continuous adjustment during testing. Parameter values provided here were then directly transmitted via the radio transceiver to the Xavier computer on board the WR, enabling the testing personnel to adjust the control parameters of the WR directly from the access point on the LC, thus simplifying the work of testing and tuning the regulating system.

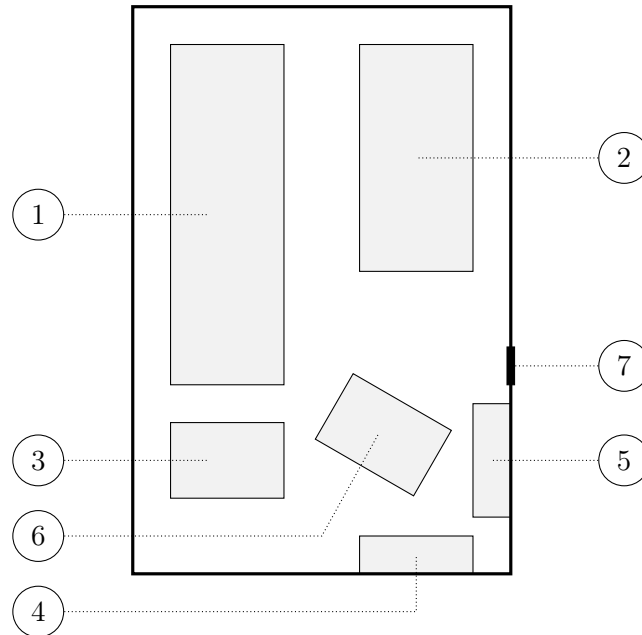


Figure 10: Schematic overview of hardware system installed in the portable box used on the LC. 1: Lithium battery, 2: Satlab GPS, 3: Voltage regulator, 4: NodeMCU WiFi board, 5: STM32, 6: Holybro radio transceiver, 7: Coaxial connector for GPS antenna.

## 2.7 Communication protocols

To communicate between the different components, a hardware protocol had to be selected. Several established protocols exist and the candidates for communication were USART, SPI, and  $I^2C$ .

Each of the aforementioned protocols have advantages as well as disadvantages over the others and therefore a careful elimination criteria was used to select a protocol based on simplicity, reliability as well as putting into consideration the capability of the available hardware components to communicate across the protocol.

The USART protocol was chosen for both the LC and WR hardware components mainly because both GPS devices could communicate through it, and the Nucleo-F303K8 micro controller is capable to communicate using the same protocol. USART was also favourable due to the reduction of cables needed to establish a physical connectivity between the devices. Furthermore, the radio unit could also be connected using the same protocol, thereby enabling full-duplex communication between the WR and LC without the need for external components.

Because the DbW system uses CAN protocol for communication between all its hardware components extensively, it was decided that the outgoing control signals generated would be on transferred across the same protocol.

## 3 Navigation

The autonomous abilities of the WR depend upon the functional properties of a computerized navigation system. Through this system, the positional data obtained by the system sensors is interpreted and processed, with the purpose of generating adequate, continuous reference data for use within the internal control system. The purpose of this section is to describe how the system is constructed and works.

The navigation system is divided into three main parts. The first part, presented in Section 3.2, investigates methods of map projection, transferring the positional data obtained by the GPS into a local coordinate system. The second part, presented in Section 3.3, describes the generation of a continuous reference path along which the system is meant to navigate and finally, Section 3.4 describes the underlying principles and the algorithms designed to guide the WR appropriately along the given path.

### 3.1 Method

The construction of the navigation system and its internal subfunctions consisted of literature reviews of similar applications which are described in the sections below.

### 3.2 Map Projection

The purpose of map projection is to make approximate conversion from global positioning data (longitude and latitude) to local coordinates in a two-dimensional coordinate system [12]. Projection of the GPS data into a local, two-dimensional system has the potential of facilitating most of the subsequent calculations and simplifying the interpretation of data in general. It will, however, leave a projection error, though, this error was considered to be neglectable. Since the WR navigation system can be assumed to run only within reasonably small areas and short travelling distances, the approximations required for this projection are assumed to be negligible.

A number of different methods of map projection, with various accuracy properties and levels of complexity, are available for potential implementation within the navigation system [12]. In this application, the Universal Transverse Mercator (UTM) was selected for implementation. This projection method divides the global surface area into 60 different area zones, each representing 6 degrees of longitude, and flatten these into a two-dimensional area [13].

### 3.3 Path Generation

The reading of position and orientation provided by the GPS sensor on the LC consists of a number of discrete data samples at a given sample rate. After being transformed (see Section 3.2) these coordinates are stored as a queue on the WR's computing device. The list of stored data obtained by the GPS unit on the LC, presented in Section 2.4.1, therefore results in a discrete representation of the path traveled by the LC. The algorithms required by the WR navigation system, in turn, call for a continuous path for several of their calculations to function smoothly. Hence, a continuous, representation of the sampled path is required.

The generation of a continuous path from discrete samples, or guide values, can be implemented through several different methods of various complexity. A smooth differentiable path could potentially contribute to a more stable regulated system with softer, continuous signal variations and less rapid changes in both reference and control signals. Due to the relatively high sample frequency of the GPS, adjustable up to 2Hz, this type of advanced smoothing algorithms was not considered to be necessary. Instead, the continuous path is constructed by linear interpolation, generated between subsequent coordinates.

### 3.4 Path Following

The generation of reference data used by the WR in order to follow the approximated travelling path of the LC (see Section 3.3) at a preset distance, is achieved by calculation of two main reference values. The first value is the distance between the two vessels following the calculated path, and functions mainly as a reference to control the WR's velocity. The second value concerns the direction of the WR, and is generated by calculating a desired direction of the WR, in order to approach and follow the calculated path in a desired manner. This reference value serves as a main indicator for the steering control of the WR. The calculations providing these respective values are described in Section 3.4.1 and Section 3.4.2 that follows.

#### 3.4.1 Distance from WR to LC

Adaptive cruise control is a well established method for automatic speed control implemented in, for example, modern vehicles. The basic task of this control system is to adjust the vessel's velocity by regards of a specified target velocity, while also observing the position or velocity of an eventual vessel ahead, by which the controller is to adjust the speed in order to maintain a secure, relative distance[14].

In the case of the WR, the system was intended to follow the track of the LC, while maintaining a constant, distance specified by a system target value. This target distance was specified so that the WR was estimated as capable to halt without risk of colliding with the LC in case of a sudden stop or rapid deceleration (see Section 5.3).

This is where the queue from Section 3.3 and the target coordinate from Section 3.4.2 come to use. The array the distance between two points,  $p_1 = (p_{1x}, p_{1y})$  and  $p_2 = (p_{2x}, p_{2y})$  can be calculated as:

$$x = \text{norm}(\mathbb{V}) = \sqrt{(p_{2x} - p_{1x})^2 + (p_{2y} - p_{1y})^2} \quad (1)$$

Where  $p_2$  comes after  $p_1$ , and  $\mathbb{V}$  is the vector from  $p_1$  to  $p_2$ . After doing this for all the points in the array the distance from the WR to the LC can be calculated using the following equation:

$$d_{LC} = x_{\text{target}} + x_{\text{rest}} + \sum_{i=1}^n x_i \quad (2)$$

Equation 2 is visualized in Figure 11. The  $x_{\text{target}}$  is the length of the  $\mathbb{G}$  vector from Table 2.  $x_{\text{rest}}$  is the distance between the target point and the coordinate  $B$  (see Figure 13). The

last term is the sum of all the vectors between the remaining GPS points in the array, calculated in Equation 1.

When  $d_{LC}$  was calculated it resulted in discrete values because the GPS sends out data with a given sample rate between every position. This will result in a constant measurement error depending on the interval in which the LC:s GPS position can be sampled, and that interval will be limited to either the GPS on the LC or the radio module communicating between the two vessels. This frequency was 2Hz for the GPS, which was the slower of the two components.

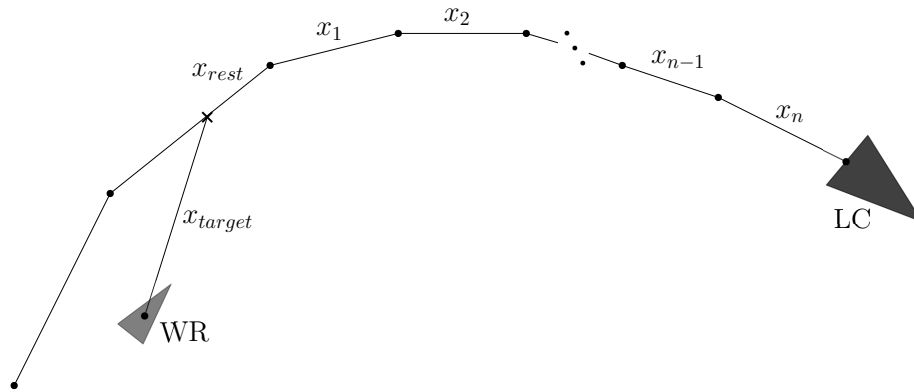


Figure 11: Distance to LC illustration.

### 3.4.2 Direction of the WR

The error that needs to be minimized for the path following is the distance between the WR and the path (see Figure 12). Since the WR can't move sideways the only way to minimize this distance is to rotate the WR towards the path. This is done trough changing the nozzle angle while producing thrust, initializing a rotating movement.

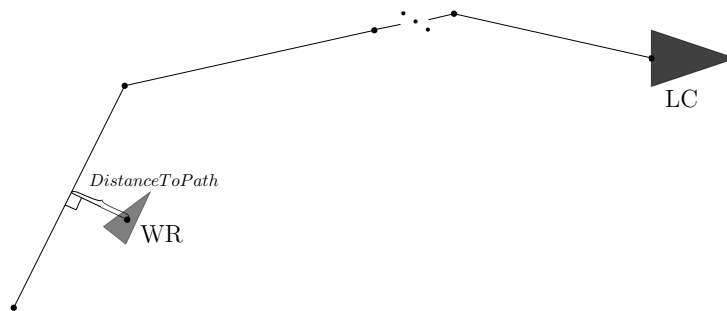


Figure 12: Perpendicular distance between the WR and the path.

A pre-constructed path following algorithm was implemented in order to calculate the required change of heading [15]. The algorithm regards the WR as an object described by three internal aspects - velocity, direction and location. The current velocity vector

of the WR is multiplied with a set time constant ( $\Delta t$ ) to get a predicted location. This coordinate is then projected on to the path of the LC, which gives a known coordinate on the LC's path. By multiplying the current velocity ( $v$ ) and  $\Delta t$  again from that point in the direction of the path the "target"-coordinate ( $G_{wr}$ ) is acquired (see Figure 13).

The algorithm could be described with the following steps:

1. Determine the WR's predicted location ( $L_{wr}$ ) with constant  $v$  and heading ( $\psi$ ).
2. Locate the closest coordinate perpendicular on the path from the  $L_{wr}$ .
3. Move this coordinate further along the path to get the  $G_{wr}$ .
4. Determine the angle between the WR's direction vector ( $\mathbb{D}$ ) and the vector from the WR to the target ( $\mathbb{G}$ ).

To determine the angle that the WR needs to rotate the following formulas are used, Table 2 contains the notations and Figure 13 visualizations:

Table 2: Variables used in the section.

Variable	Unit	Explanation
$v$	m/s	Velocity of the WR
$\psi$	rad	Angle of $\mathbb{D}$
$\mathbb{D}$	(x,y)	Direction vector of the WR
$P_{wr}$	(x,y)	Current coordinate for WR
$L_{wr}$	(x,y)	Predicted coordinate of the WR after $\Delta t$ with current $\psi$ and $v$
$G_{wr}$	(x,y)	Target coordinate for the WR
$\mathbb{G}$	(x,y)	The vector from $P_{wr}$ to $T_{wr}$
$\alpha$	rad	Angle of $\mathbb{G}$
$A$	(x,y)	Coordinate on the path, the dots in Figure 13
$B$	(x,y)	Another coordinate after A on the path
$\Delta t$	s	Constant sample time
$\mathbb{P}$	(x,y)	Vector from $A$ to $P_{wr}$
$\mathbb{B}$	(x,y)	A help vector between $A$ and $B$
$C$	(x,y)	The perpendicular point on the path from $L_{wr}$
$\mathbb{C}$	(x,y)	A help vector between $A$ and $C$
$\gamma$	rad	The desired rotation of WR

$$\mathbb{D} = (\cos \psi, \sin \psi)$$

$$L_{wr} = P_{wr} + v \cdot \Delta t \cdot \frac{\mathbb{D}}{|\mathbb{D}|}$$

$L_{wr}$  is thus calculated from the current WR position ( $P_{wr}$ ),  $v$  and scaled with  $\Delta t$  (see Figure 11).

$$\mathbb{P} = P_{wr} - A$$

$$\mathbb{B} = B - A$$

The closest point to  $L_{wr}$  on the path is

$$C = A + \frac{\mathbb{P} \cdot \mathbb{B}}{\|\mathbb{B}\|^2} \cdot \mathbb{B}$$

and consequently the target which the WR is aiming for is

$$G_{wr} = C + v \cdot \Delta t \cdot \frac{\mathbb{B}}{\|\mathbb{B}\|}$$

By taking the closest perpendicular point on the path from the predict location and the same velocity vector as before but with the direction of the path the target point is found.

The vector to the target is then

$$\mathbb{G} = G_{wr} - P_{wr}$$

having the direction ( $\alpha$ )

$$\alpha = \arctan \frac{\mathbb{G}_y}{\mathbb{G}_x},$$

which gives a desired rotation ( $\gamma$ ) of the WR

$$\gamma = \psi - \alpha.$$

These equations show the concept of how the desired rotation,  $\gamma$ , is calculated when there is only a path with two points. In the real path there will be several points and then the algorithm needs to find the closest vector where the WR is and keep track where the LC is moving. In the implemented algorithm there is a queue (see Section 3.3) that keeps track of the order in which the LC's coordinates have been generated, even if the algorithm searches for the closest point on the path. For example, if the LC has done a U-turn and the path on the way back is closer to the WR, the WR would still use the earliest generated coordinate, causing it to follow the LC's path.

If either  $L_{wr}$  or  $G_{wr}$  is placed further along on the path than  $B$  (see Figure 13) the same method is applied on the remaining part of the vector, extending from  $B$ . Meaning that no matter the velocity difference between the WR and the LC at any time,  $G_{wr}$  will always be a point on the path.

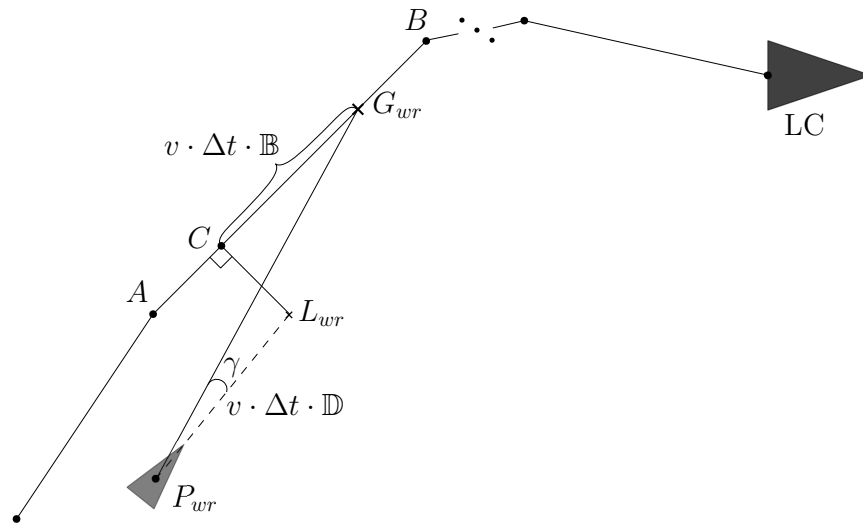


Figure 13: Direction calculation illustration.

### 3.5 Output

The navigational algorithms work together to provide two essential control signals to the control system. These signals are the change of heading  $\gamma$  and the distance to the LC  $d_{LC}$ . The control system will then calculate signals for throttle and nozzle angles which are transmitted across a CAN bus to the actuators to actuate the desired change.

## 4 Model

A model for simulation was derived in order to verify the path following algorithm and the control system. This chapter describes the method used to derive the model, how the model works, and what tests were performed to improve the model.

### 4.1 Method

Simulink and MATLAB were used as the environment in which the model was created. The model was sequentially constructed, adding one degree of freedom (DoF) was added at a time. This was done in such a way that the deceleration effect to a complete stop was simulated against the model and when the results were satisfactory enough, the next degree of freedom was added. This process was repeated until enough degrees of freedom were obtained.

For the next step, simulation of a propulsion force was modeled. The WR is propelled by a jet stream produced by an Internal Combustion Engine (ICE). An equation describing how such a jet behaves was built and then configured until it produced similar behavior as the WR.

### 4.2 Coordinate Systems

To fully describe the motion of a watercraft, such as a PWC, six DoF are required [16]. These include the movement along the three axes  $x$ ,  $y$  and  $z$  and the rotations  $\omega_x$ ,  $\omega_y$  and  $\omega_z$  about the axes (see Figure 14). Depending on the context, the number of degrees of freedom can be reduced, thus simplifying the model. In maneuvering theory (the control of ships moving in relatively calm water) it is common to adopt a model with three DoF, taking into account the movement along the  $x$  and  $y$  axes (called surge and sway respectively), and the rotation about the  $z$  axis (called yaw) (see Figure 3). These naming conventions [16] and the variable names chosen to represent these degrees of freedom are given in Table 3.

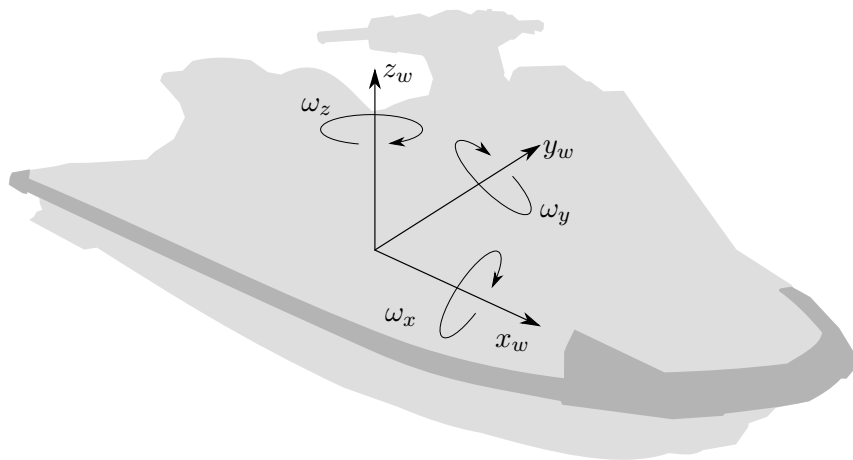


Figure 14: Axes local to the WaveRunner.

Table 3: Names and variables for the 3 degrees of freedom used in the modeling of the WR.

Name	Linear/angular vel	Pos & euler angle
surge	$V_x$	$x$
sway	$V_y$	$y$
yaw	$\omega_z$	$\phi$

Furthermore, it facilitates to use two different coordinate systems: one fixed to the body (the vessel) one fixed to the earth (see Section 3.2). Different frames for the earth-fixed coordinate system can be chosen; here a North-East-Down frame is used, in which the area surrounding the vehicle is approximated with a plane, meaning, Earth is approximated to be flat [16]. Following the notation used in [16], the body-fixed coordinates will be subscripted with  $w$  and the Earth-fixed coordinates will be subscripted with  $e$ .

### 4.3 Equations of Motion

The equations of motion of the WR are based on Newton's second law

$$m \cdot \frac{dv}{dt} = \sum \mathbb{F}$$

where  $\mathbb{F}$  in this particular case consists of the thrust  $\mathbb{T}$  of the nozzle and the WR's resistance  $\mathbb{R}$ .

A model describing the motion of the WR according to these equations were implemented in Simulink (see Figure 15). Each DoF was represented using a separate subsystem. Values for all constants used in this section are given in Table 4.

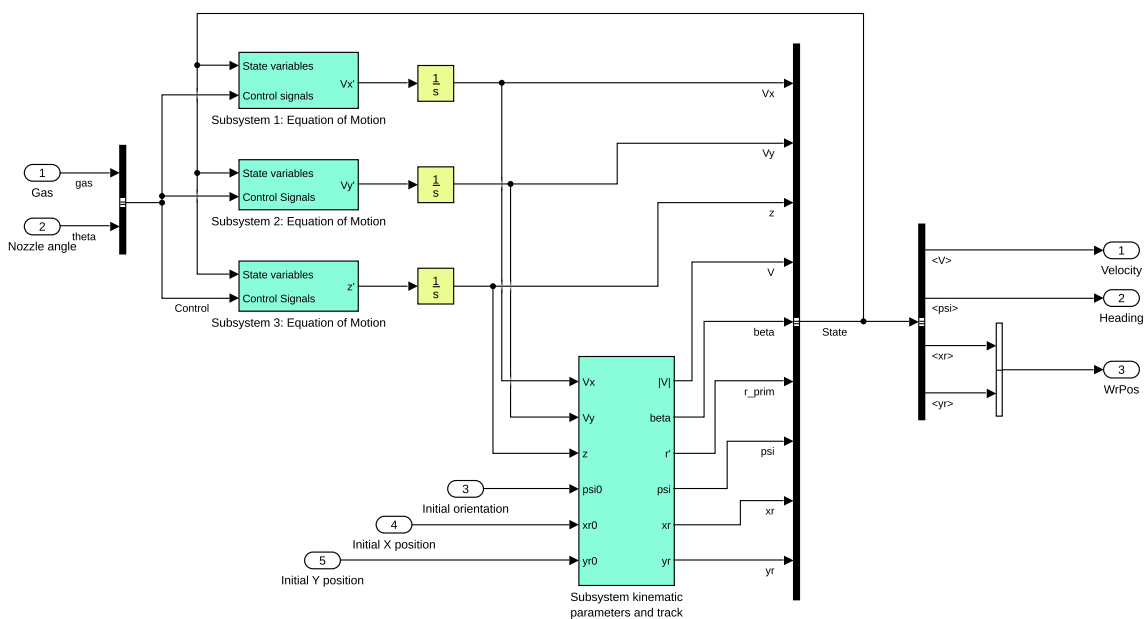


Figure 15: Simulink model of the WaveRunner.

Table 4: Constants and their values used in the modelling of the WR.

Constant	Value	Unit
$c_r$	-4	-
$\rho$	1.025	kg/L
$a_l$	1	m <sup>2</sup>
$p_2$	3.0166	Pa
$a_o$	0.005	m <sup>2</sup>

### 4.3.1 General Equation of Resistance

According to [17], the resistance of a water craft can be described with the equation

$$R = c_r \cdot \frac{\rho}{2} \cdot V^2 \cdot a_l$$

where  $c_r$  is resistance coefficient specific for the vessel being modelled,  $a_l$  is the lateral area of vessel submerged into water,  $\rho$  is the density of the water and  $V$  is the velocity of the vessel. The area of the WR in contact with the water is not constant: increased velocity will result in less area submerged into water. To take this into account,  $a$  was approximated to  $a = \frac{a_l}{1+v}$ ,  $a_l$  being the lateral area in contact with water at rest.

### 4.3.2 General Equation of Thrust

The propulsion system in the WR is a jet discharge system: a reactive force is created by discharging water at a high rate through a nozzle. Following the simple model for a jet propulsion system as described in [18], the reactive force  $\mathbb{T}$  can be written as

$$\mathbb{T} = \rho \cdot q \cdot (v_2 - v_1)$$

where  $v_1$  is the velocity of the jet,  $v_2$  is the velocity of the water flowing out of the jet and  $q$  is the volumetric flow out of the jet.  $v_1$  is approximated as being equal to the velocity of the WR;  $v_2$  can be expressed as

$$v_2 = \sqrt{\frac{2 \cdot (p_1 - p_2)}{\rho}}$$

where  $p_1$  is the pressure before the jet and  $p_2$  is the ambient pressure in the water surrounding the jet.  $p_2$  is given the constant value of the pressure of salt water at 0.3 m depth,  $p_1$  is approximated as being linearly related to the throttle  $\lambda$ . The flow volume out of the jet  $q = a_o \cdot v_2$  is a linear scaling of the flow velocity out of the jet where  $a_o$  is the orifice area of the nozzle. The Simulink model implementing the thrust subsystem is presented in Figure 16.

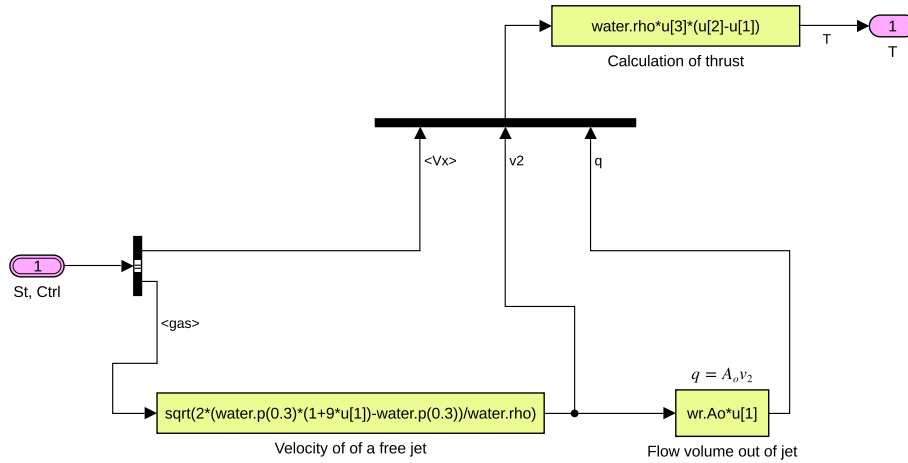


Figure 16: Simulink subsystem for thrust from a jet.

### 4.3.3 Equation of Surge Motion

The surge component of the collected forces acting on the WR can be determined by taking the surge component of the thrust  $\mathbb{T}$  and the resistive force in the surge direction. For the thrust, a simple distribution of force based on the nozzle angle was used, resulting in the surge thrust  $T_x = \|\mathbb{T}\| \cdot \cos \delta$ .  $\delta$  is the nozzle angle (see Figure 17). The resistive force  $R_x = R$  as this was used as the basis for the derivation of the resistance.

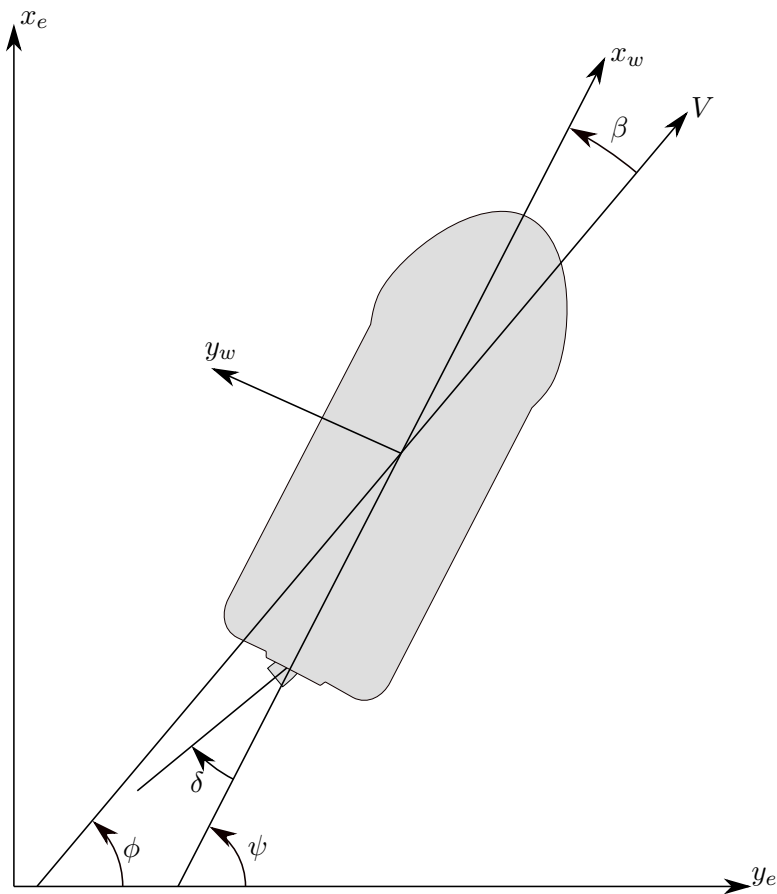


Figure 17: WR angle and Nozzle angle.

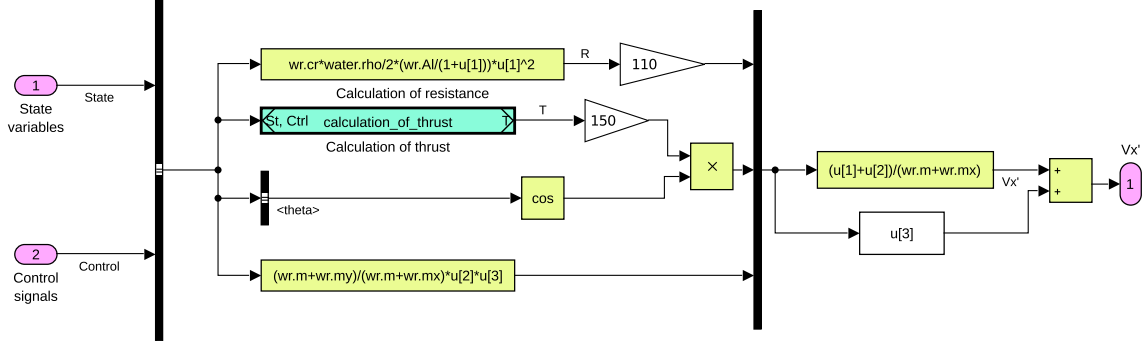


Figure 18: Simulink subsystem for surge motion.

The surge component of the force is also affected by the other components. E.g. when the WR initiates a rotation (i.e., yaw motion  $\omega_z$ ), momentum from the sway direction ( $v_y$ ) is transferred via inertia to the surge direction ( $v_x$ ). The resulting equation of motion is

$$\dot{v}_x = \frac{m + m_y}{m + m_x} \cdot v_y \cdot \omega_z + \frac{R_x + T_x}{m + m_x}$$

where  $m$  is the total mass of the WR and eventual passengers, and  $m_x$ ,  $m_y$  are the added masses due to the inertia of water. The Simulink model is depicted in Figure 18.

#### 4.3.4 Equation of Sway Motion

There is no positive force acting in the sway direction, only the force of resistance has to be taken in account. Added to this is the transmitted velocity from the other components. The resulting equation is thus

$$\dot{v}_y = \frac{m + m_x}{m + m_y} \cdot v_x \cdot \omega_z + \frac{R_y}{m + m_y}$$

#### 4.3.5 Equation of Yaw Motion

The yawing component of the force consists of the resulting moment of the thrust. The reference point has been assumed to be the center of the WR, giving the thrust moment  $T_z = \|\mathbb{T}\| \cdot \sin(\delta) \cdot \frac{L}{2}$  where  $L$  is the length of the WR and  $\delta$  is the nozzle angle (see Figure 17). The equation for the yawing motion is then

$$\dot{\omega}_z = \frac{T_z}{I + I_z}$$

where the moment of inertia  $I$  is calculated by approximating the WR as an ellipsoid with the axis through the center.

#### 4.3.6 State Variables Subsystem

A separate subsystem was written to calculate state variables based on the equations of motion. These were used in the simulation to track current position of the WR relative to a fixed coordinate system. The subsystem is depicted in Figure 19.

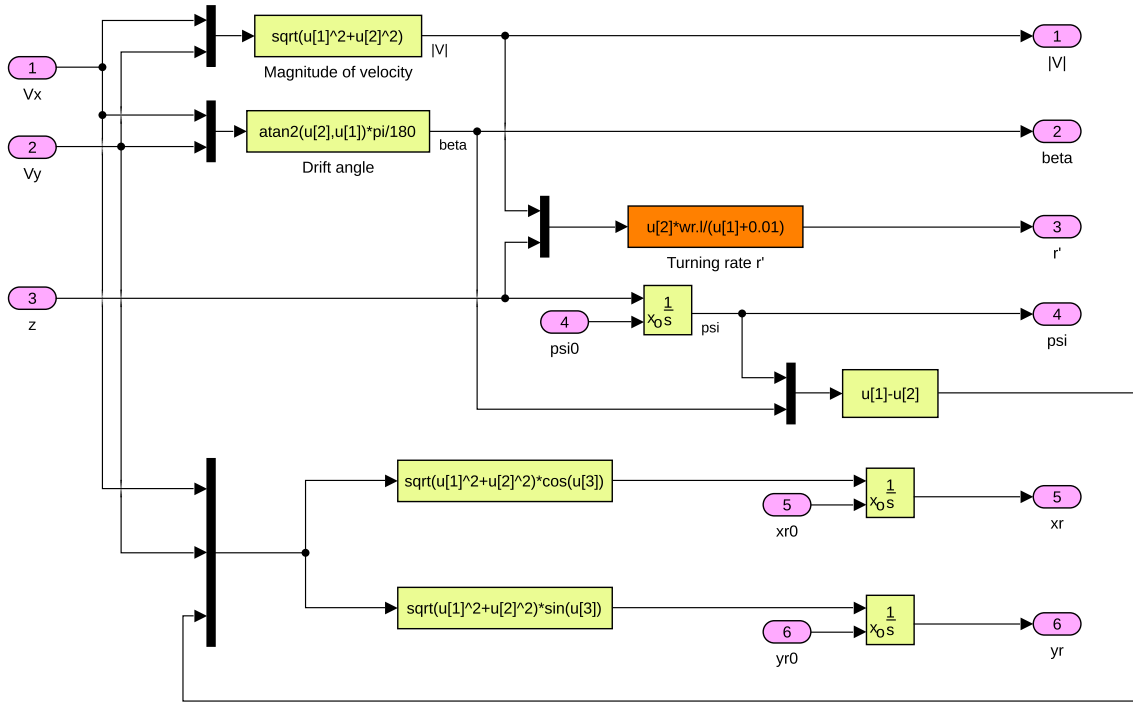


Figure 19: Simulink subsystem for kinematic parameters.

#### 4.4 Verifying Model

To ensure realistic behavior from the model real life tests had to be made. The main focus of the tests were to acquire data for coasting stops, acceleration, and steering which could then be used to improve the model's equation of motion parameters. The tests were run in cooperation with SSRS at their station in Långedrag, Gothenburg.

The tests were conducted with two individuals on board the WR, one operating the vehicle while the other handled the telemetry equipment and radio communication with personnel at shore. As for data acquisition two units were used; a battery powered GPS unit logging data to a SD-card, and an Arduino board reading and storing signals from the throttle. These two logs were then spliced and merged using a custom built Python script.

In total six parameters were tuned using the test data, which can be found in Table 5. These parameters functions as uniform scaling for the surge, yaw, sway thrust and resistance in the Equations of motions presented in Section 4.3.

Table 5: Parameters tuned to test data.

Resistance		Thrust	
Variable	Meaning	Variable	Meaning
$r_x$	Resistance along x	$t_x$	Scaling of thrust along x
$r_y$	Resistance along y	$t_y$	Scaling of thrust along y
$r_z$	Rotational resistance about z	$t_z$	Scaling of torque about z

#### 4.4.1 Scaling of Forwards Momentum

At first the model was restricted to only one direction,  $x$ , in order to improve  $r_x$  and  $t_x$ . A series of coasting stops and acceleration runs were performed and documented to later be plotted along with the simulation data. A multitude of values for  $r_x$  and  $t_x$  was iterated through until the plots shared a common appearance, final values  $r_x = 110$  and  $t_x = 150$  were used (see Figure 20 & 21).

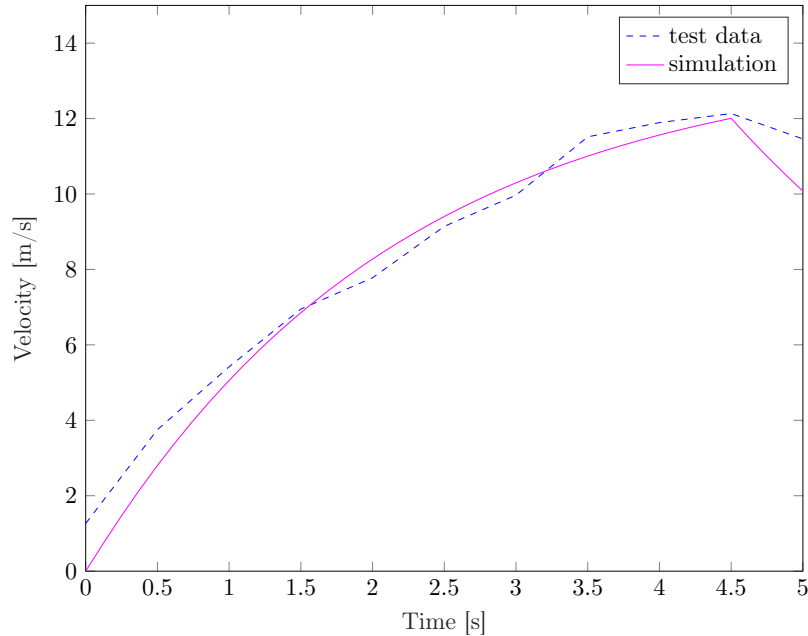


Figure 20: Plot for acceleration, showing test and simulation data with  $r_x = 110$  and  $t_x = 150$ .

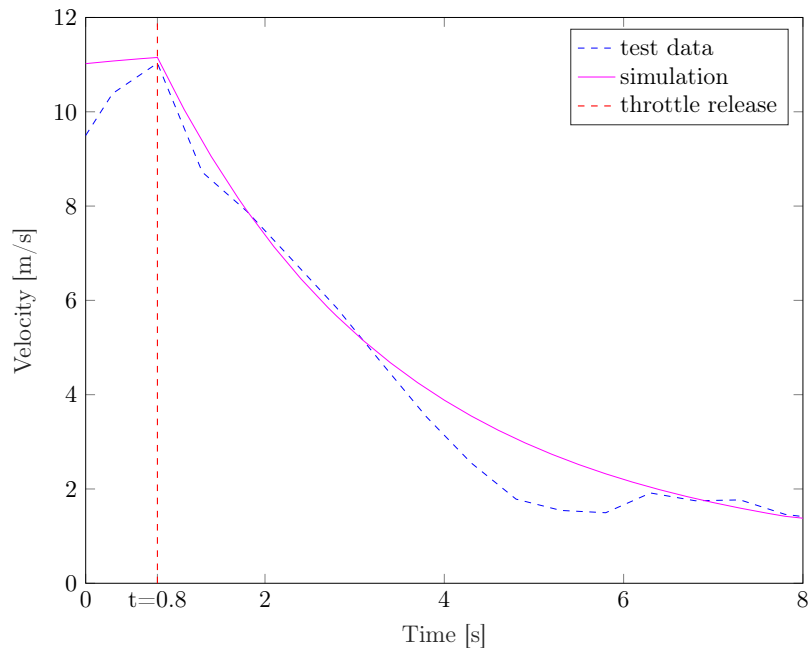


Figure 21: Plot for coasting stop, showing test and simulation data with  $r_x = 110$  and  $t_x = 150$ .

The results, while not an exact match, were deemed acceptable.

#### 4.4.2 Scaling of Rotational Resistance and Thrust

Scaling of rotational parameters,  $r_z$  and  $t_z$ , were tuned next. To do this a series of test runs with constant throttle and steering angle were executed. The collected data was plotted in MATLAB along side a simulated run with the same inputs. As with the scaling for parameters in the  $x$ -direction, different values were tried until an acceptably close match was achieved.  $r_z = 8$  and  $t_y = 25$  were used as final values (see Figure 22).

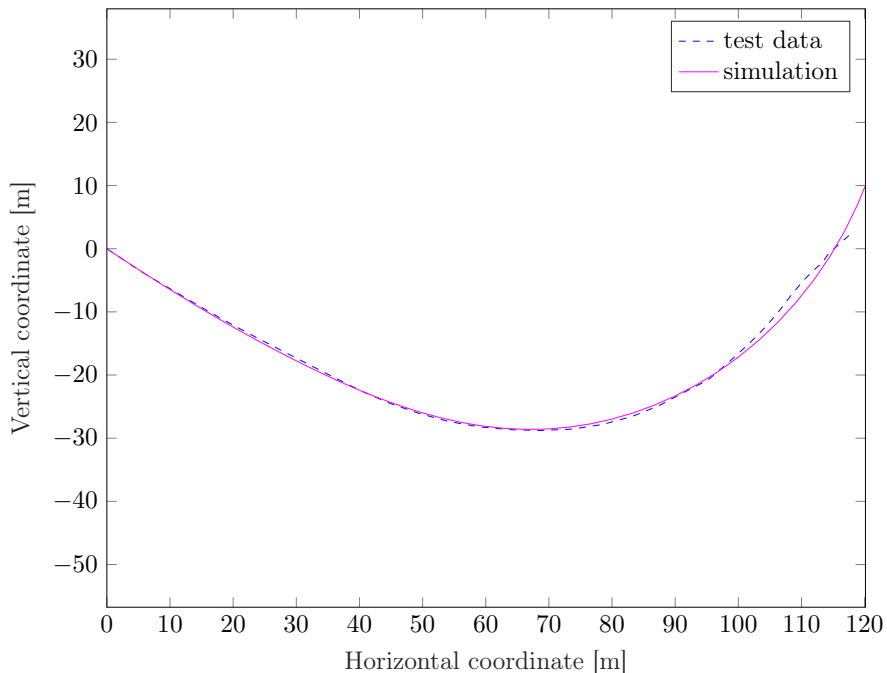


Figure 22: Test and simulation data from steering test. Scaling factors used:  $r_z = 8$  and  $t_y = 25$ .

#### 4.4.3 Scaling of Lateral Resistance and Thrust

In Section 4.2 it was described that 3 DoF was recommended when producing a model for a ship operating in calm sea. However, when experimenting with the lateral resistance and thrust it was found that these factors proved to have a very small impact on the final results. Thus, both  $r_y$  and  $t_y$  was set to equal zero to reduce model complexity.

## 5 Control System

The purpose of the control system is to handle continuous control of two parameters, throttle ( $\lambda$ ) and nozzle angle ( $\delta$ ). This is done by the use of the output values calculated in Section 3, namely the heading change ( $\gamma$ ) which is used as control deviation while calculating  $\delta$ , and the distance between the vessels ( $d_{LC}$ ) used as a feedback value for  $\lambda$ . This section presents the properties of the implemented feedback loops and their internal regulators, as well as the methods of parameter tuning and system improvements achieved by system simulation.

### 5.1 Method

The first step in developing a control system for the WR was to produce a simple model of transfer functions in the Laplace plane. The ICE of the WR was modeled as a first order transfer function, determining the force produced at a given throttle value. The force was then, due to it being directed by the nozzle, split into two components, one for driving the WR forward and the other to rotate the WR. Two additional transfer functions were needed, one to control the forward momentum of the WR and one for controlling its rotation.

After the simple model was built, feedback loops were introduced, in combination with a controlling unit. To begin with these control units were proportional, P, controllers. The control systems were tested individually to verify functionality. The forwards controller was tested by trying out a couple of straight line runs with varying velocity, then the rotational controller was tested by following a path veering back and forth, while keeping constant velocity. When both controllers reacted as expected the proportional controllers were replaced by complete proportional, integral and derivative (PID) controllers.

The settings of the controllers were thereafter tested by computer simulation using the navigational algorithms (see Section 3) and the simulation model (see Section 4), and each respective parameter was adjusted in accordance with the result. The controllers were first modeled in MATLAB and Simulink, and thereafter reconstructed in C++ to be able to run in real time on the Xavier computer on board the WR.

### 5.2 Overall Control System

Two actuator systems on the WR provide the possibility of electronic control of steering and thrust. The first one is the throttle system, which regulates torque produced by the ICE. The second is a step motor, which controls the steering shaft, and thereby turns the nozzle at the back of the WR. The input values for these actuators were distributed through a CAN databus, and constitute the final control signals of the regulating system.

The control system is designed with the focus of minimization of two main deviations. The first one consists of the deviation from the set target distance between the LC and WR, similarly to an adaptive cruise controller (see Section 3.4.1). The second consists of the distance that the WR has deviated from the path (see Figure 2).

In order to acquire both errors, two feedback loops were needed. The first feedback loop controls the actual distance from the WR to the LC along the path as determined in Section 3.4.1. Due to the fact that the WR is incapable of performing collateral maneuvers, the shortest distance to the path cannot be controlled in itself. Instead the control system

was designed to try to minimize the heading deviation ( $\gamma$ ) which in turn would result in a reduction of the distance to the path.

Both control systems use discrete time controllers due to the fact that they are handling discrete signals while computing. The controller for distance used a PI-controller while the one for steering used a PD-controller.

### 5.3 Throttle Control

The actuator for the throttle requires an input value between 0 to 100, where 0 represents no throttle and 100 represents full throttle. This system is controlled using the actual distance to the LC along the path and the set reference value for how far behind the LC the WR should be (see Figure 23).

The reference value was set to be constant, i.e. 55 m, because of two factors. Firstly, the wake behind the LC generally provides calmer water which is beneficial for the control system due to the reduction of external disturbance, meaning that better performance can be achieved if the WR is close to the LC. Secondly, a safe distance was desired to ensure no collisions during testing, thus 55 m was used as a compromise between safety and performance.

To determine the error ( $d_e$ ) in distance behind the LC, the feedback loop uses the actual value and the reference value, i.e.

$$d_e = d_{LC} - d_r$$

The controller used in this control system was a PI-controller because the system did not have a natural integrating property, causing a small error to persist. An integral anti-windup, with a saturation of 0-100, was also used due to the fact that if the WR was too close to the LC when it started, the integral term of the controller would accumulate a significant negative value. The anti-windup prevents an overshoot term when the error crosses over to positive values again [19].

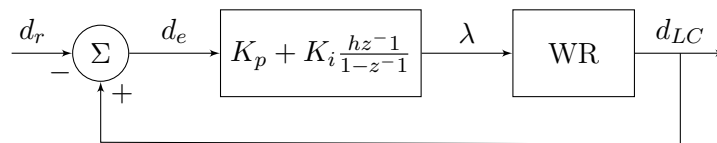


Figure 23: Throtte control system.

### 5.4 Steering Control

To move the WR closer to the path it has to rotate; in this case the error was determined by the algorithm in Section 3.4.2 because it uses the WR's actual direction and the direction from WR to the target (see Figure 24). The differences between the two directions was the error  $\gamma$  in direction. There is no need for an integral property in this controller, due to the fact that the reference value for the controller was an angle while the actual output was a change in angular velocity, causing the controller to exhibit a natural integral property. Therefore, the chosen controller for the steering was a PD-controller. The need for a derivative part is due to the quick changes in desired rotation. The derivative part

amplifies changes of the error, resulting in a more responsive turning behaviour. A filter is applied on the derivative term to reduce signal noise. Finally the control signal value,  $\delta$ , was saturated to  $-24^\circ$  to  $24^\circ$  to conform with the limitations of the real nozzle movements.

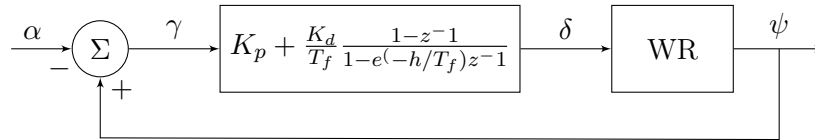


Figure 24: Steering control system.

## 5.5 Implementation

The control system presented in this section and the path following algorithm described in Section 3 were implemented in C++ . The language was chosen due to its rich diversity of open source libraries, its integration with SIMULINK, its ability to easily interface with hardware, and its object-oriented nature, making development of big projects more feasible than e.g. C.

To ease the development, a few libraries were used. The library Eigen 3.3.7 [20] was chosen for the linear algebra calculations used in the path following algorithm. For the map projection (see Section 3.2), the decision was made to use Proj4 version 5.2 [13]. Further, a low pass filter library [21] was incorporated.

## 5.6 Simulation

Parameter values for the controllers were determined through iterative simulation. In this subsection that process will be explained as well as why certain decisions regarding the controller design was made, such as why a low pass filter was used and how the output was scaled to work with a greater range of velocities.

In all simulations, Simulink was used as the interface (see Figure 25). This set up mirrors the real life system which was implemented with the Xavier computer, represented by the Path Following / Control system block, while the WaveRunner model block represents the WR and its dynamic reaction to water. The Xavier block contains the two controllers and the navigational algorithms (see Section 3), and the model block utilizes the simulation model (see Section 4) to simulate the physical attributes of the WR in motion.

The Xavier block gathers data from its four inputs, situated on the right hand side of the block. These inputs consists of LC coordinates, which are sent with a set interval, and state data for the WR. The WR state data consists of three sets of sub-data; position, angle, and velocity. The Xavier in its turn gives three output signals; Throttle, Nozzle angle, and Test. Throttle and Nozzle angle are sent to the model block whereas Test is only used to monitor different values during simulation.

Using the model as a reference, control system variables were tried until an authentic WR path, captured during trial at Långedrag, was able to be recreated. The results can be seen in Figure 29, containing an overview of the simulated runs, the deviation of the WR to the path, the total distance to the LC, output signals, and WR's velocity and heading. The first set of parameters for the produced control system are presented in Table 6.

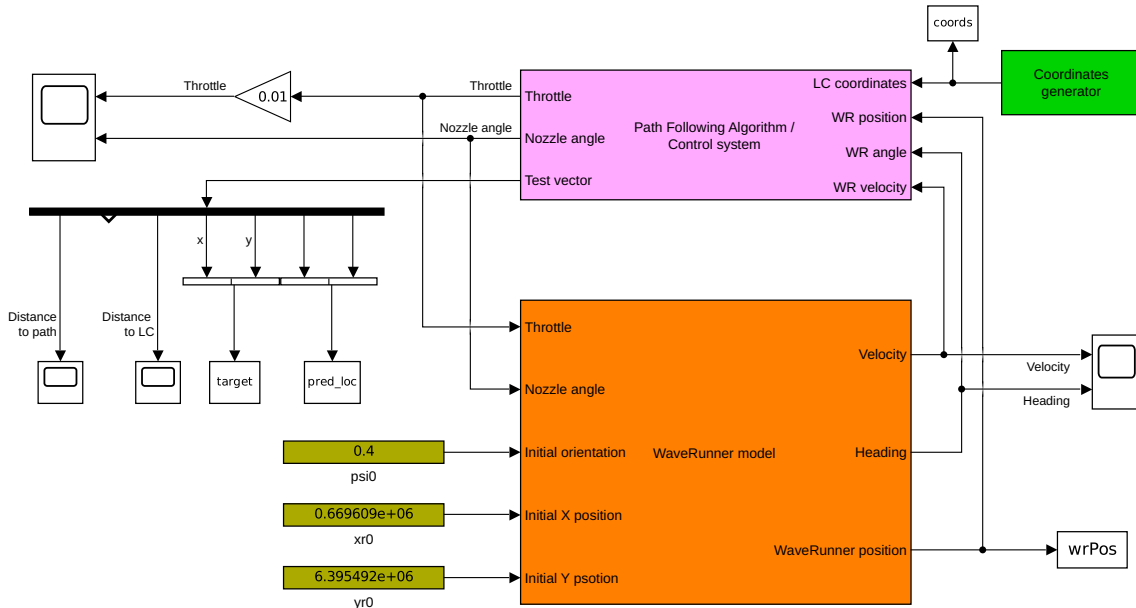


Figure 25: Simulation set up in Simulink.

Noteworthy is that the nozzle velocity was restricted to the interval of  $-12^\circ$  and  $12^\circ$ . This was done for safety precautions, not wanting the WR to perform harsh turns.

Table 6: The control parameters for simulation used in Figure 29, 30 & 31.

$\Delta t = 2$	Throtte	Nozzle
Kp	5	-0.01
Tf	1	0.9
Kd	0	-1.4
Ki	5	0
Max	100	$12^\circ$
Min	0	$-12^\circ$

Simulations were run at varying velocity, while still using the same path in order to increase robustness for the controllers. In Figure 30 the velocity was set to twice the original speed used in the first simulation run. In this figure it is evident that the WR cuts corners when traveling at higher velocities, almost traveling in a straight line. The WR deviates up to 6.5 metres from the given path as seen in Figure 30b. Figure 30d also show the throttle signal containing noise.

In Figure 31, a simulation run at two thirds of the original simulations velocity is shown. As with the previous two simulations throttle control signal can be seen containing noise (see Figure 31d). Total distance between the WR and the path was considerably high (see Figure 31b), indicating that the path following worked poorly for this magnitude of velocity.

From these three simulated runs two observations were made; thrust from the engine had a major impact on steering causing the model to not be able to adapt to varying velocities, and both throttle and nozzle angle control signal contained noise.

In order to combat the two problems, not handling varying velocities and the occurrence of a noisy control signals, two solutions were implemented. The first one was to include thrust as a component in the steering controller, and the second was to introduce low pass filters on both control signals. This can be seen in the updated control systems (see Figure 26 & 27).

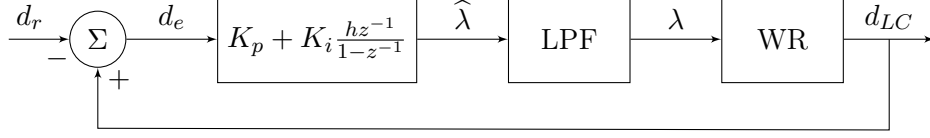


Figure 26: Throttle control system.

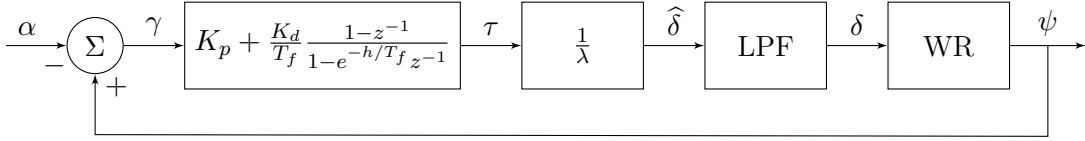


Figure 27: Steering control system.

The relationship between the thrust and nozzle angle was designed as a geometrical one (see Figure 28). With nozzle angle before low pass filtering ( $\hat{\delta}$ ) depending on the original control signal ( $\tau$ ) and the throttle control signal ( $\lambda$ ) which is linearly related to rotational generating thrust ( $\mathbb{T}_Z$ ).

The relation between throttle and steering is non linear due to the occurrence of a sinusoidal component (see Equation 3), thus a linearization of the steering was implemented (see Equation 4 & 5). This was possible because of the restriction set on  $\hat{\delta}$  to the interval of  $-24^\circ$  to  $24^\circ$ , thus the approximation  $\hat{\delta} \approx \sin \hat{\delta}$  was made.

$$\tau = \lambda \cdot \sin \hat{\delta} \quad (3)$$

$$\tau = \lambda \cdot \hat{\delta} \quad (4)$$

$$\hat{\delta} = \frac{\tau}{\lambda} \quad (5)$$

The second problem, regarding the noisy control signals were solved by using low pass filters on both signals. The noise on the throttle control signal occurs because the distance to the LC updates discretely with a low sample frequency. When a new coordinate was generated the distance increased rapidly, causing the signal to spike. To solve this a first order low pass filter was added to the control signal to filter out the high frequencies. The sample frequency ( $\omega_s$ ) used to generate the coordinates is  $4\pi$  rad/s. A low pass filter with cutoff frequency ( $\omega_{co}$ ) of  $2\pi$  rad/s was used to filter out this noise. Using this  $\omega_{co}$  means that the noise will be canceled while not affecting actual velocity changes.

As for the nozzle angle control signal, the noise was less severe than the one found for the throttle. The cutoff frequency for this filter was set at higher 3 Hz due to the steering output expecting more rapid fluctuations in control signal.

With the implementation of the improved controllers, the parameters had to be tuned again (see Table 7 for updated values).

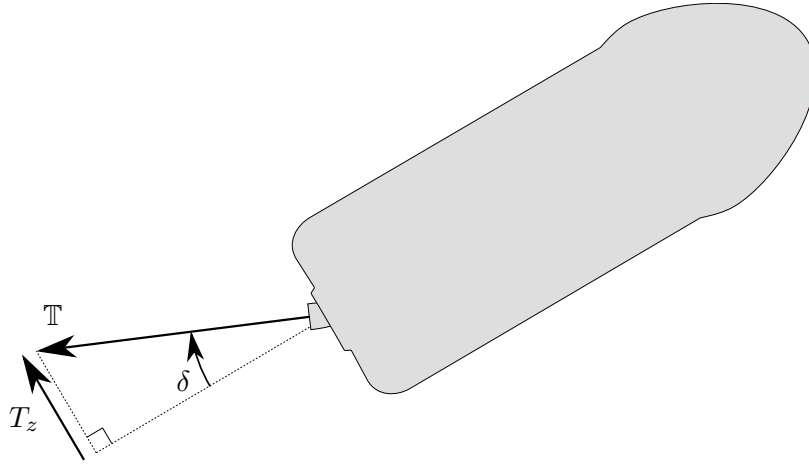


Figure 28: Thrust from the nozzle and its components.

Table 7: The control parameters used in Figure 32, 33 &amp; 34.

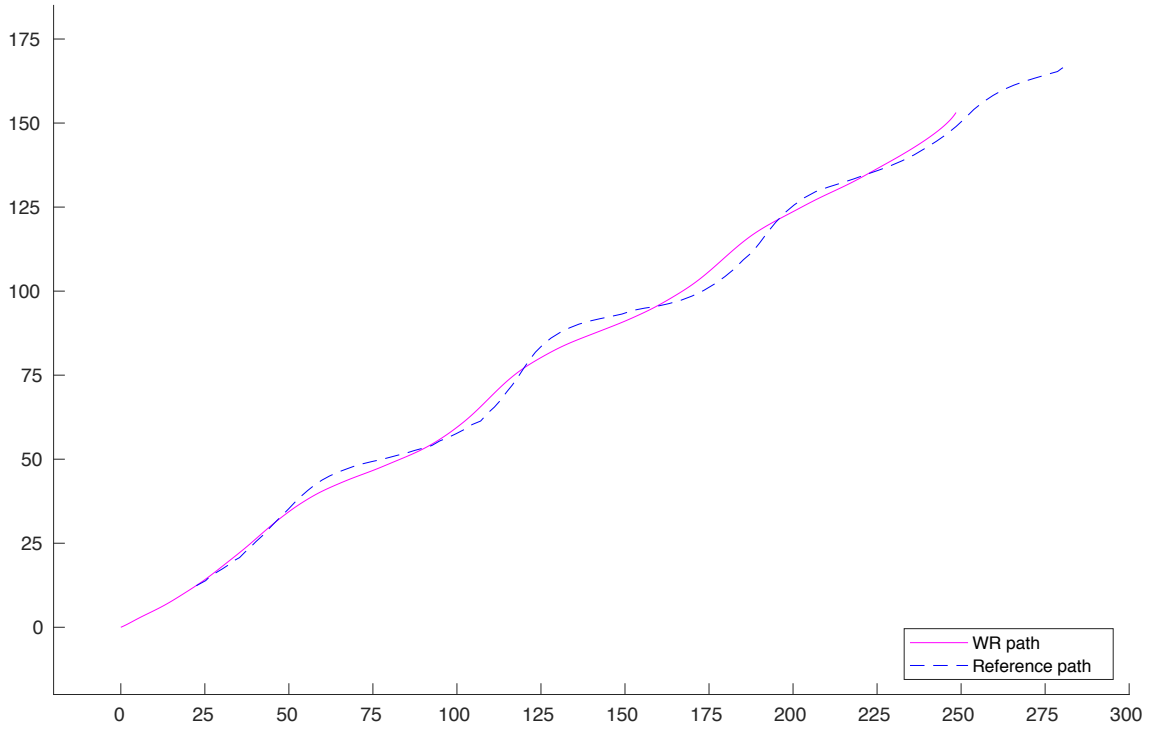
$\Delta t = 2$	Throtte	Nozzle
Kp	4	-1
Tf	5	1
Kd	0	-100
Ki	5	0
Max	100	18°
Min	0	-18°
$\omega_{co}$	1	3

To verify improved performance of the new controller and their parameters three additional simulations were run using the same path and velocity variations as previously (see Figure 32, 33 & 34).

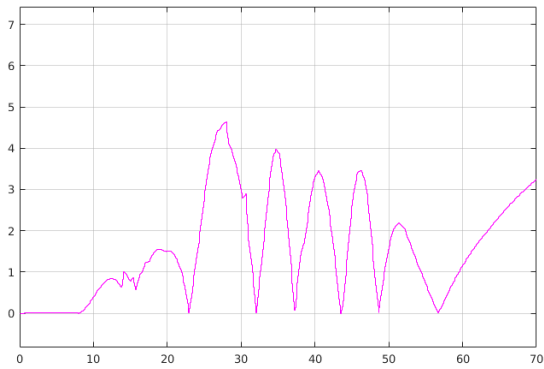
The revised simulations using the updated controllers show improved performance. The distance between the WR and the path has been reduced for lower velocities (see Figure 32b & 34b). As for the higher velocities, no immediate improvement can be seen (see Figure 33b). This is likely due to the fact that the WR is trying to catch up to the LC, which has a head start on the WR. To reduce this distance the WR tries to yet again cut corners (see Figure 33d & 30c). This result is not to significant, since the path and velocity combination is not realistic. With the increased velocity in the simulation of the real life run the path should also have deviated form the original. The noise has been reduced for both control signals in all three simulations (see Figure 32d, 33d & 34d).

The distance to the LC has not been increased by much by the implemented changes. This is likely due to the fact that low pass filter only removed the noise and not the essential frequencies.

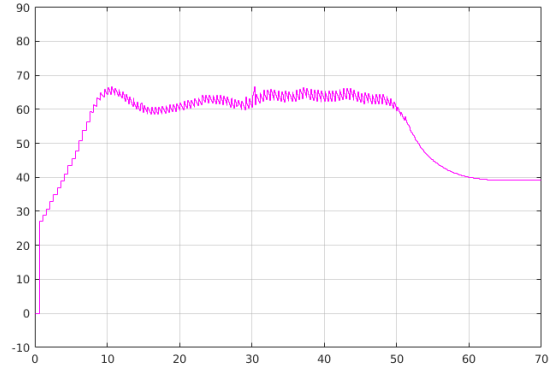
The control system appears to operate stable; the simulations show that the subsystems developed, navigational and controlling, work together to make the WR follow a LC. The control parameters produced in this section, using the model from Section 4, are only meant as a baseline and field tests needs to be performed to assert good final performance.



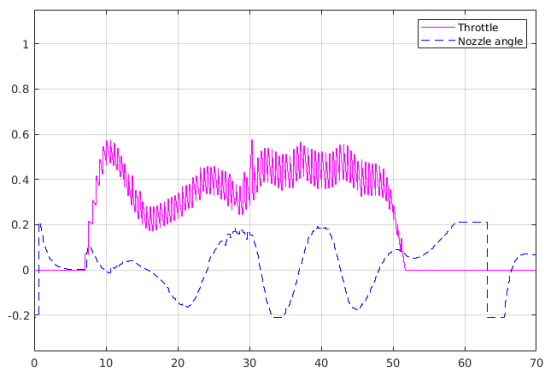
(a) Birds eye view showing simulated path for WR following a test path. All axis are given in meters.



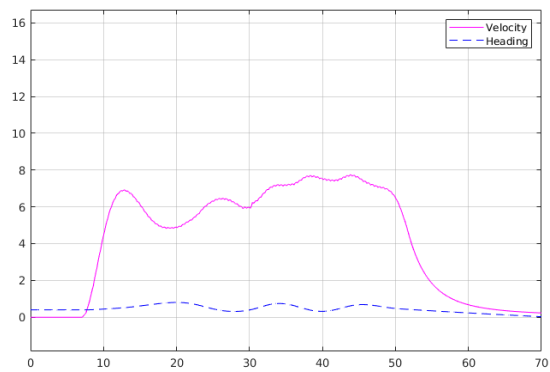
(b) Distance between the WR and the path in meters over time.



(c) Distance between WR and LC in meters over time.

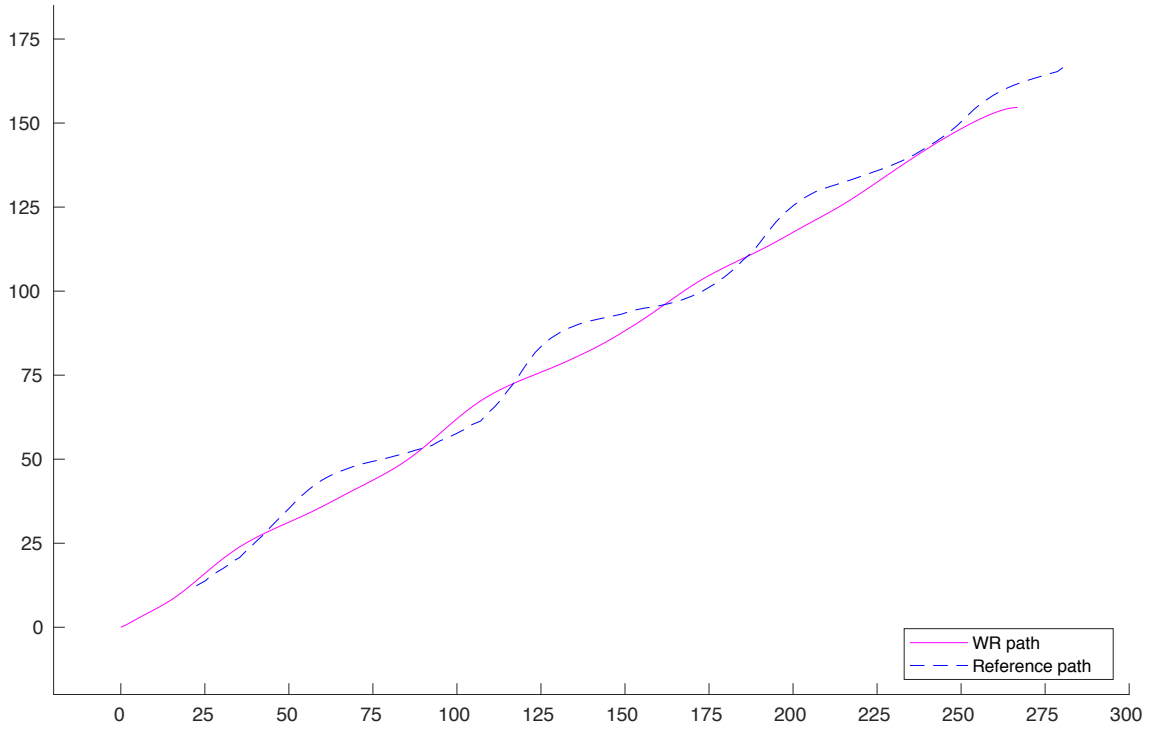


(d) The control signals over time, the throttle signal is scaled by 0.01.

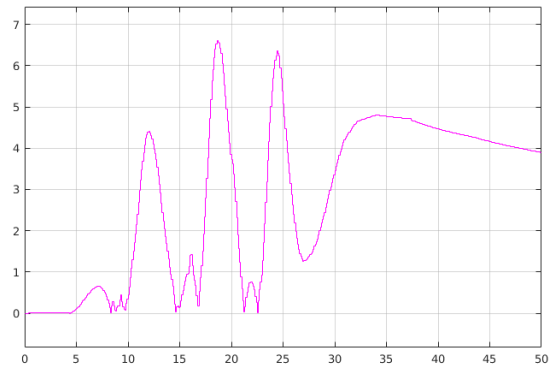


(e) WR's velocity in m/s and heading in rad over time.

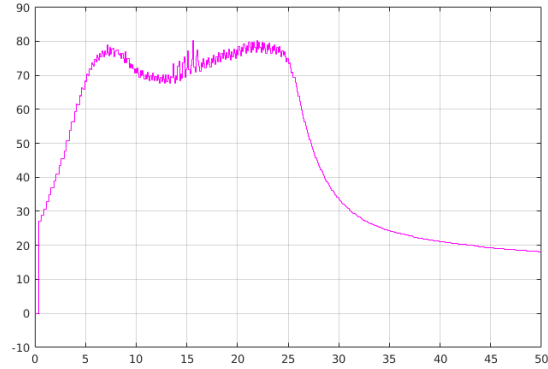
Figure 29: Simulation run using original velocity.



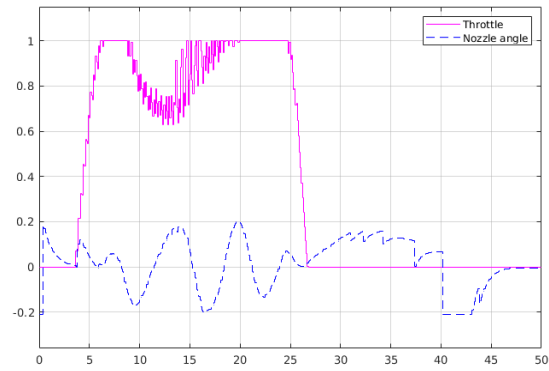
(a) Birds eye view showing simulated path for WR following a test path. All axis are given in meters.



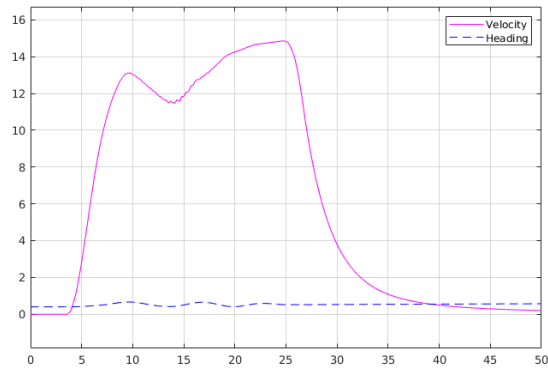
(b) Distance between the WR and the path in meters over time.



(c) Distance between WR and LC in meters over time.

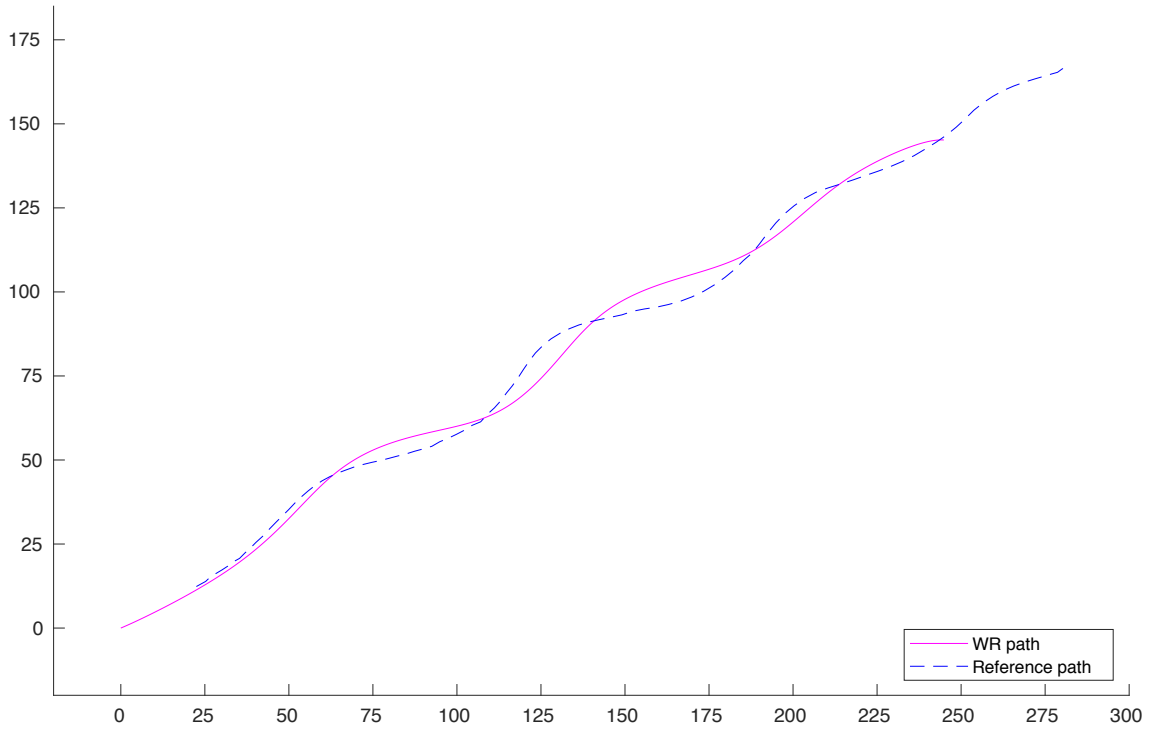


(d) The control signals over time, the throttle signal is scaled by 0.01.

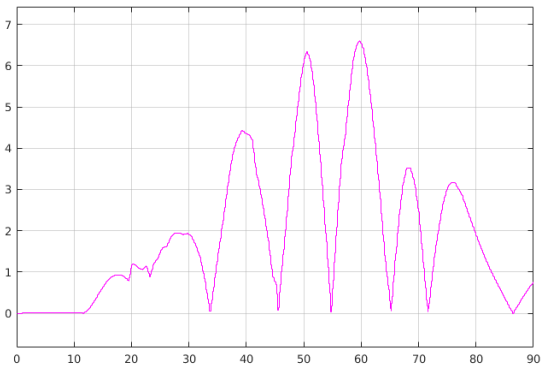


(e) WR's velocity in m/s and heading in rad over time.

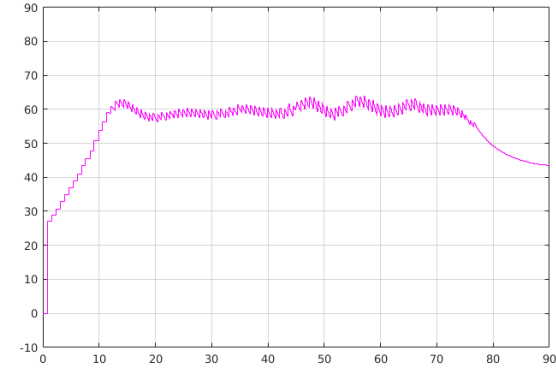
Figure 30: Simulation run with two times the original velocity.



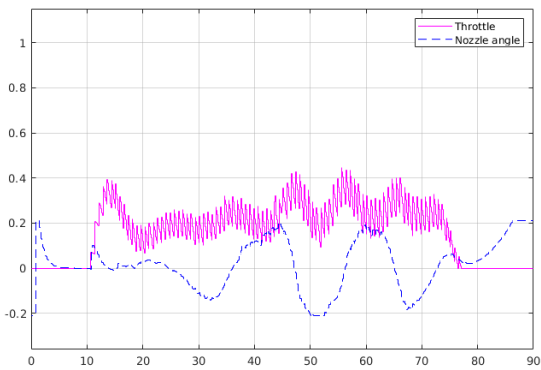
(a) Birds eye view showing simulated path for WR following a test path. All axis are given in meters.



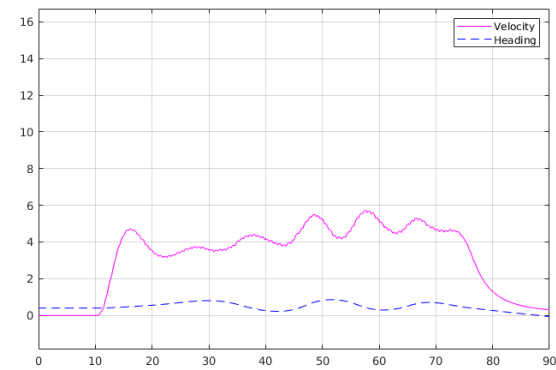
(b) Distance between the WR and the path in meters over time.



(c) Distance between WR and LC in meters over time.

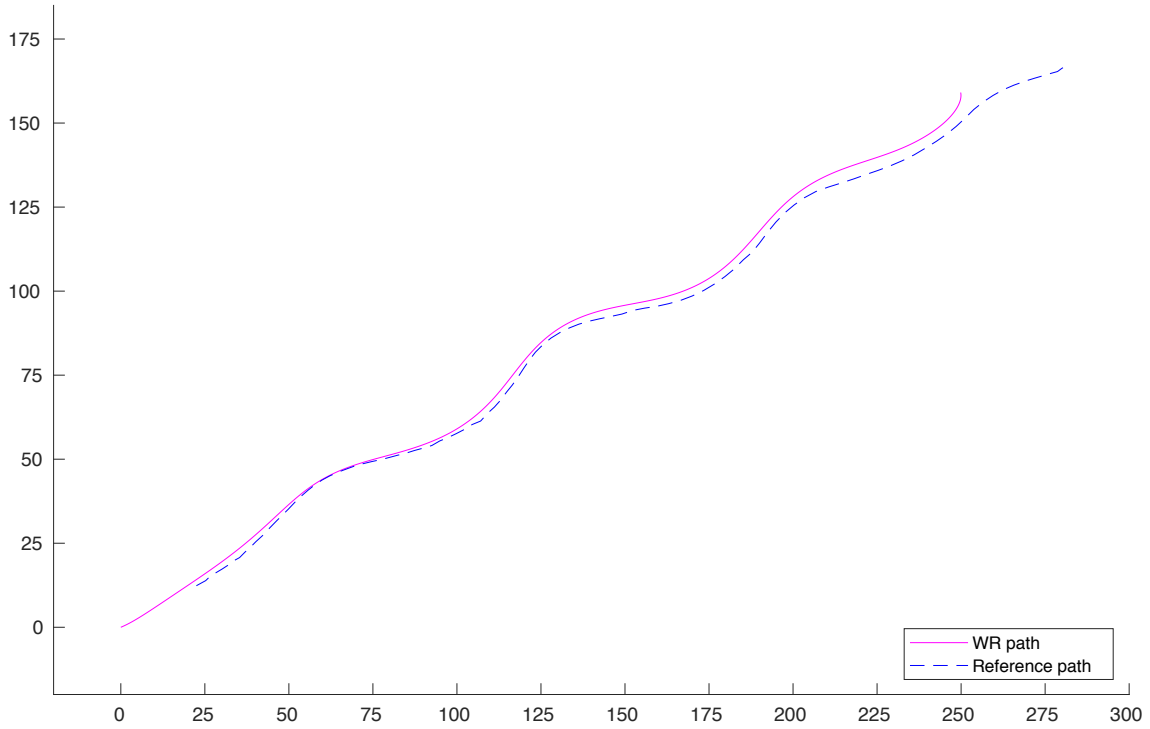


(d) The control signals over time, the throttle signal is scaled by 0.01.

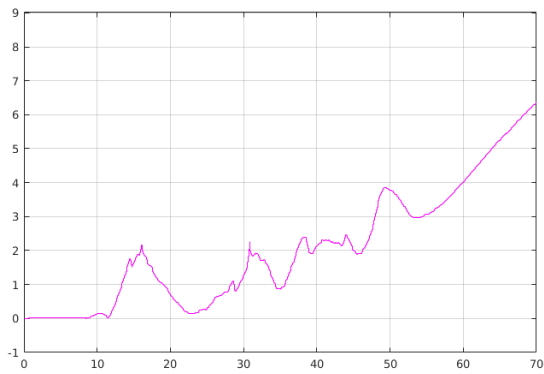


(e) WR's velocity in m/s and heading in rad over time.

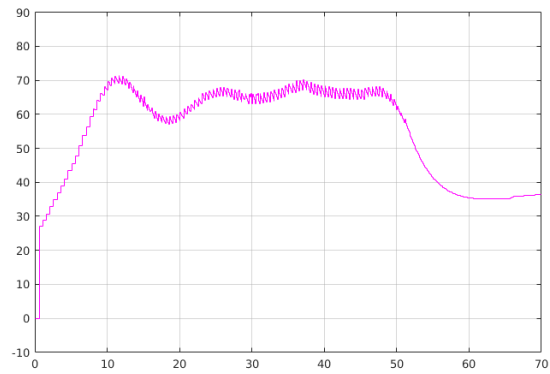
Figure 31: Simulation run with two thirds of the original velocity.



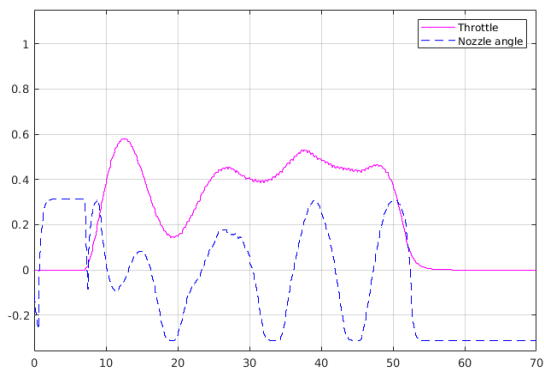
(a) Birds eye view showing simulated path for WR following a test path. All axis are given in meters.



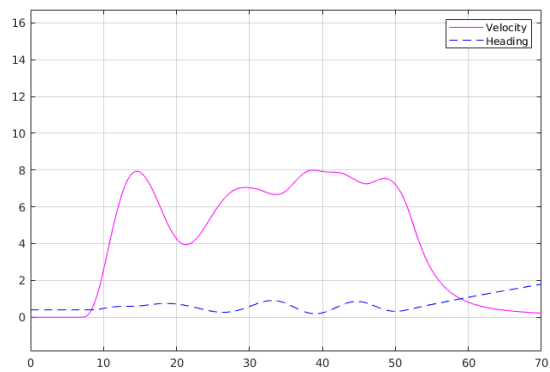
(b) Distance between the WR and the path in meters over time.



(c) Distance between WR and LC in meters over time.

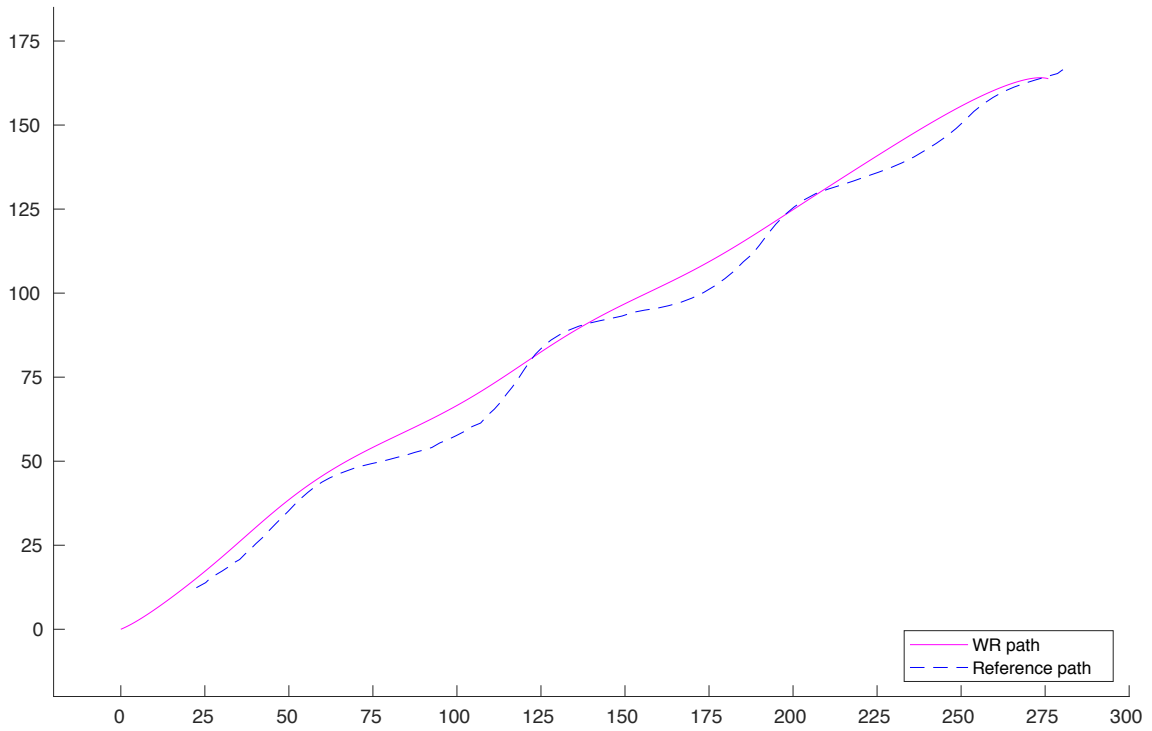


(d) The control signals over time, the throttle signal is scaled by 0.01.

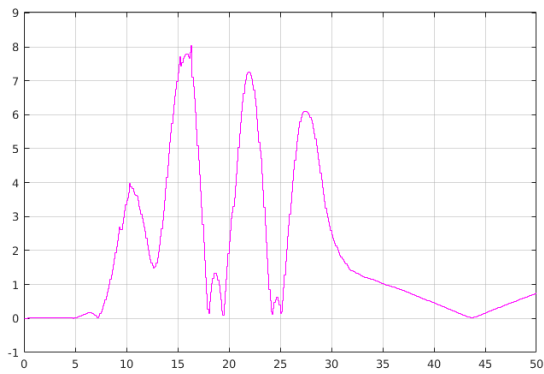


(e) WR's velocity in m/s and heading in rad over time.

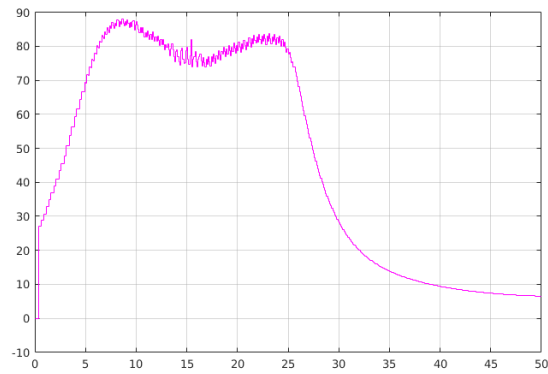
Figure 32: Simulation after corrections, run using original velocity, with filter and  $\frac{1}{\lambda}$  applied.



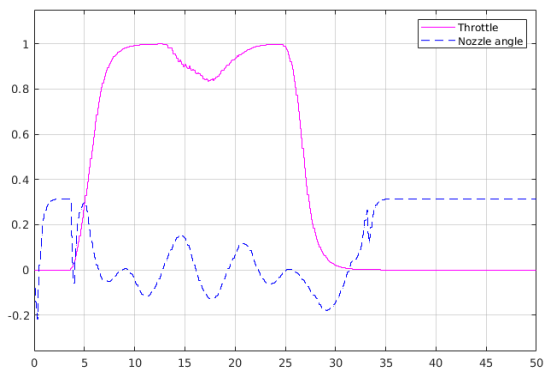
(a) Birds eye view showing simulated path for WR following a test path. All axis are given in meters.



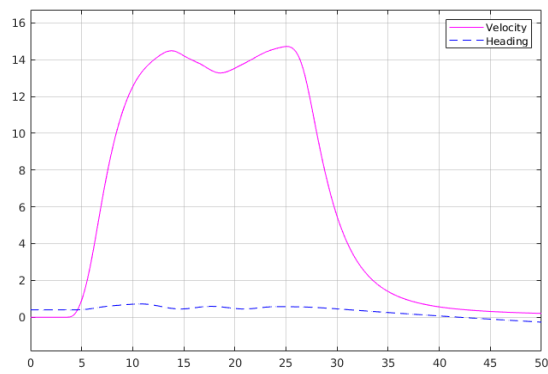
(b) Distance between the WR and the path in meters over time.



(c) Distance between WR and LC in meters over time.

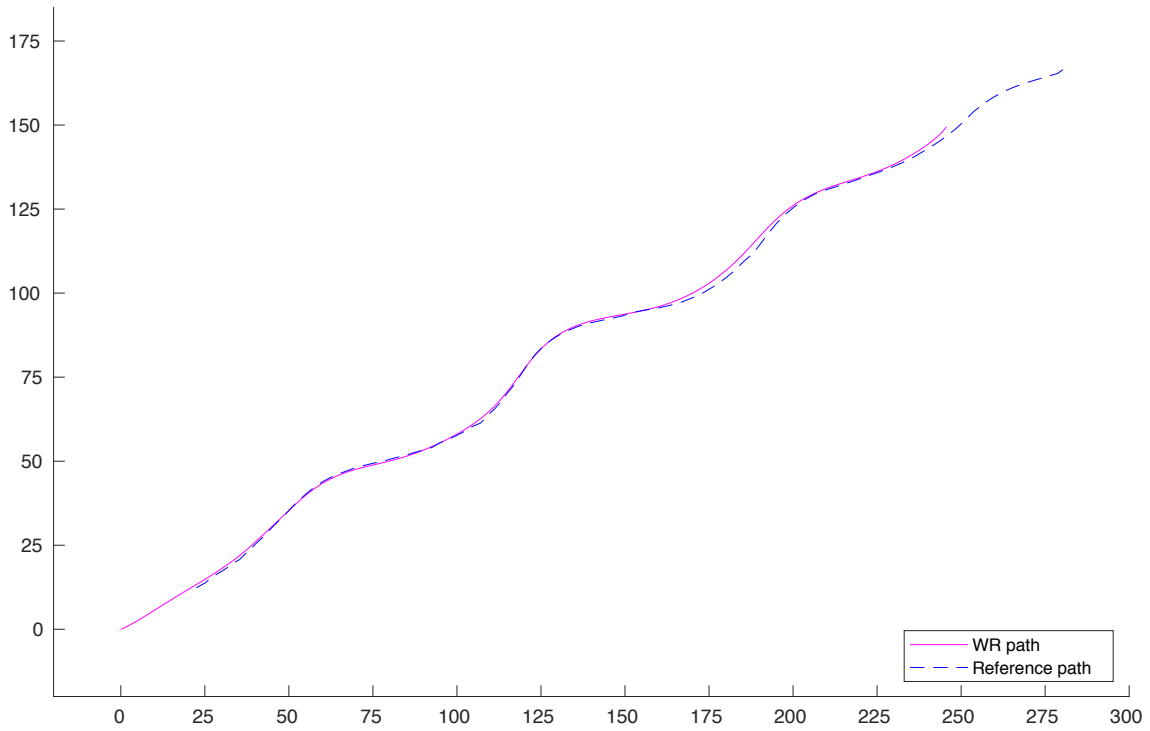


(d) The control signals over time, the throttle signal is scaled by 0.01.

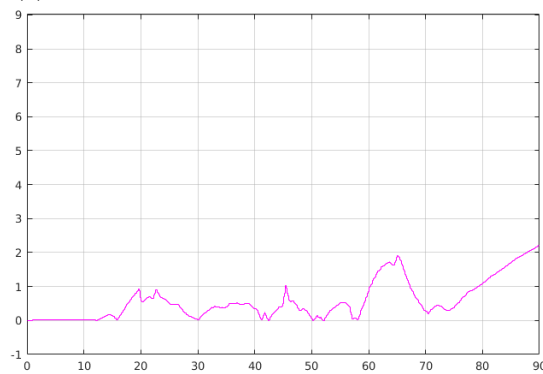


(e) WR's velocity in m/s and heading in rad over time.

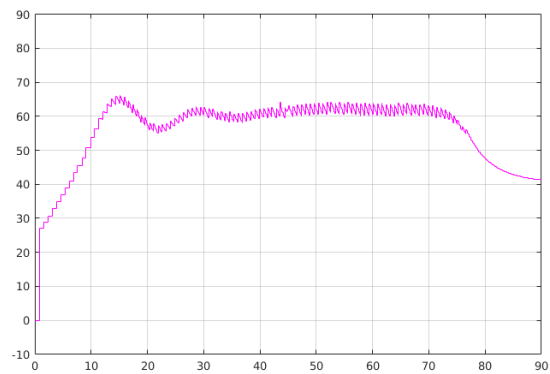
Figure 33: Simulation after corrections, run with twice the original velocity, with filter and  $\frac{1}{\lambda}$  applied.



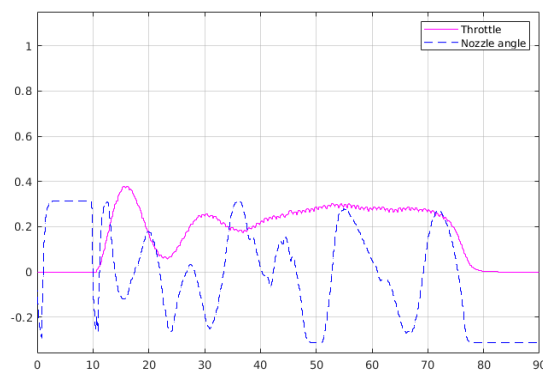
(a) Birds eye view showing simulated path for WR following a test path. All axis are given in meters.



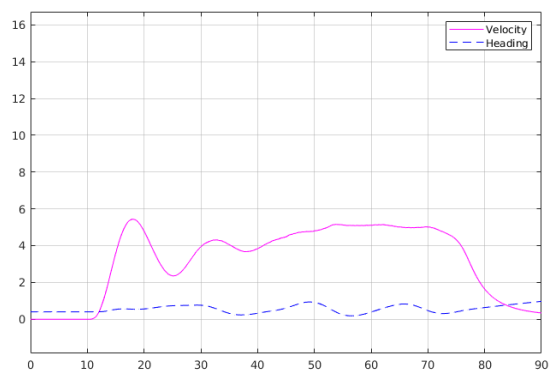
(b) Distance between the WR and the path in meters over time.



(c) Distance between WR and LC in meters over time.



(d) The control signals over time, the throttle signal is scaled by 0.01.



(e) WR's velocity in m/s and heading in rad over time.

Figure 34: Simulation after corrections, run with two thirds of the original velocity, with filter and  $\frac{1}{\lambda}$  applied.

## 6 Discussion & Conclusion

This section is to present an evaluation of the methods and results achieved within the project, as well as suggestions for further development of the system. The section also provides final project conclusion and presents results achieved.

### 6.1 Discussion

The purpose of this section is to provide an evaluative image of the methods utilized and developed within the project, as well as the results produced or achieved herein. A number of different compromises of various degree were made during the execution of the project, due to several prerequisites, factors and constraints regarding both time and complexity. These compromises are also to be presented and discussed within this section.

The methods applied during the system construction and design phase can be found only partially covering the standard procedures of system construction. The construction phase did not include any comprehensive investigation and comparison of different system layouts, and the studies of specific hardware solutions were only conducted briefly. These investigating parts of the project thus stand the risk of being found inadequate. The main reason for this approach was the external system guidelines provided for the project, in accordance with the description given in the project delimitations (see Section 1.3).

The literature review, conducted during the initial phase of the project, was performed in a relatively brief fashion, and could therefore be estimated as somewhat insufficient. Several subsequent parts of the project could have been benefited by a more rigid study of previous methods and solutions, regarding cases equal or similar to the problems encountered in this project. Some of the implementations within the project could potentially have been solved using existing solution methods, instead of requiring functions and methods produced from scratch. This would have spared working time, and could also potentially result in a number of more rigid and effective solution methods. It is clear that the working methods of the project were centered around the construction of solutions a bit too early on, leaving insufficient space for the work of initial, preparatory research.

A low pass filter was used to reduce noise in the throttle signal, caused by the low sample frequency of the LC's coordinates (see Section 5). This caused the system to be less responsive to rapid changes, which could in some cases be found undesirable. This function deficiency could potentially be minimized by the use of, for example, a prediction model of the distance, e.g. use of the LC's velocity in the last coordinate to predict what the distance most likely are when not transmitting. This could be used to smooth out the variations in the calculated distance value, thus making it possible to lower the sensitivity of the low pass filter, or even remove it completely.

Due to limited possibility of field testing, the project came to rely heavily on a number of simulations, which were in their turn constructed through the studies of simplified models. This causes the results to rely highly on the accuracy of the models, although this accuracy could be estimated poorly. However, as stated in Section 5, the simulated parameter values are only supposed to be used as a baseline, meaning that the values derived during the project are intended for further calibration during field tests, which is assumed to be the case regardless of the accuracy of the simulation models.

The simplified construction of the mathematical model of the WR and its driving behavior, while ignoring several factors such as the influence of pitch and roll movements, was also

used as a baseline for the construction of the control system. The design of the control system could therefore be evaluated as a simplification. A more extensive study concerning the dynamical behavior of the WR, providing an increased accuracy for the mathematical model of the system, could also have the potential of providing a foundation for a more rigidly constructed control system. The available input data provided by the Ellipse inertial measurements of the WR carry the potential of providing real-time measurements of several reference values possible to use in this type of advanced control system. The development of a state vector based control system, and the ability of accurate verification and simulation of the system before the execution of field tests, would be highly benefited by the construction of a detailed model of the WR, studying all the 6 degrees of freedom (see Figure 3). A state vector based control system, in its turn, could potentially result in a high increase of system stability and robustness.

The Xavier computer has a maximum power consumption of 65 W, which could result in a considerable generation of heat during high performance calculations. The enclosure for this unit is small and waterproof, thus not optimized for heat dissipation. This problem was countered by use of a metal enclosure, providing a higher level of thermal conductivity, and by installing the Xavier computer so that the heat sink of the device could be connected directly to the metal casing through a thermal compound. These factors were estimated as sufficient for the conduction of shorter test runs, and the use of the computer for the less demanding program routines developed in this project. To ensure the system's ability to operate at high performance for an extended amount of time, the heat development of the system should be studied more rigidly, possibly resulting in the need for the implementation of a more efficient cooling system.

## 6.2 Future Development

In this section, a number of thoughts and ideas regarding further development of the project and its results are presented. This also includes ideas that were not implemented due to factors such as time restrictions and project delimitations. The project guidelines concerning adaptation of the system design, regarding the system's potential for further development (see Section 2.2), have been a key aspect during the entire project throughput. Thereby related aspects of further development considered throughout the project are included in the presentation below.

In its entirety, the project is developed with a potential for continuous expansion through several subsequent projects, where the abilities of the WR could be enhanced further. It would, for example, be possible to utilize the capacity of the Xavier computer for processing of larger sets of data, obtained through devices such as vision cameras, Radar or Lidar technology, and different forms of advanced data processing using methods of artificial intelligence (AI). This could potentially be utilized to improve the WR's autonomous abilities even further, making it able to interpret its surroundings and navigate more freely.

It would be desirable, in accordance with suggestions and specifications provided by the project stakeholders at the SSRS, for the WR to be able to navigate autonomously out of the harbor, while handling static or dynamic obstacles along the way. It would also be desirable for the WR to achieve the ability to autonomously dock to the leader boat in a safe manner [2]. These developments should be possible to implement through expansion of the basic system provided by this project.

Computerized systems regarding wireless or autonomous vehicle control, such as the one

studied and implemented in this project, stand a considerable risk of exposure to computer intrusion, with the aim of sabotaging or taking control of the device [22]. This aspect has been excluded from further consideration throughout the execution of this project (see Section 1.3). However, in order to ensure the secure functionality of the designed system in commercial use, the aspects of data security and intrusion prevention are in need of further studies.

Several sensors included in the current system possess a number of potentially useful abilities, which are, as mentioned in Section 6.1, not fully utilized in the current application. The Ellipse INS GPS sensor includes a number of advanced sensors for inertial measurement, which could be studied and utilized in several ways. For example, the wake behind the LC could be possible to detect using the heave, pitch and roll sensors. This data could be analyzed further, and used for example to ensure that the WR is kept within the center of the wake. The internal, extended Kalman filter of the device also comes with the ability of precise correction of the positional and directional data in cases of GPS signal outage. Further studies of these abilities, and the routines of calibration and maximization of their functionality, would be valuable for improvement of the functionality of the system.

The Satlab GPS sensor used for the acquisition of positional data regarding the LC would also have the potential of extended utilization. This mainly concerns the usage of the second GPS antenna, which could be used to acquire the directional data of the LC. This functionality remains unutilized within the current implementation, since the path generation algorithm only considers the positional data of the LC. The directional data of each sample point could be used to receive a more complete image of the movement of the LC, and make the control system able to predict factors such as water currents. It would also be possible to study the actual speed of the LC in, or between, each sample point, and include this value in the calculation of the WR's velocity and throttle control. For example, in cases when the LC slows down in order to make a sharp turn in a narrow passage, it would be desirable for the WR to do the same maneuver at the same position, instead of slowing down at the same time as the LC.

During the project execution, the functionality of the system could only be tested through computerized simulation. The system was supposed to be run through field tests, where the control system parameters would be possible to adjust further, but due to time limitations and issues concerning the hardware and communication system, this could not be done. Therefore, the system has not been sufficiently ensured to function in real applications, which would be essential. These field tests should preferably be conducted using a real LC, but could also be done by providing the system with coordinates from a pre-recorded path, delivered one by one to the navigation system. This would simulate the process of generating a path, but still make it possible to verify the main functions of the autonomous system.

As mentioned in Section 5.4, the WR simply shuts down if it gets too far away from the path or starts going in the wrong direction. This could be solved using state based controller, detecting different situations and changing behaviour to handle these. States discussed during project execution were mainly a rough sea state and one for the WR to reconnect to the wake produced by the LC when straying too far away, but this could potentially be extended much further.

The Satlab GPS device, theoretically, has a capability of responding with either ASCII or binary message formats. Using ASCII as the default format results in the communication with, and data obtained from the GPS may become difficult to handle. If, instead, the

device was configured to function using binary messages, this could reduce the complexity of the code written, thereby reducing reliability issues that can affect the functionality and stability of the system. Binary messages are cleaner, shorter and more concise, which also implies that more data could be transferred when need arises.

### 6.3 Conclusions

According to the simulated data, producing a WR that autonomously follows a LC is completely viable using GPS technology, a small computer, PID controllers, and an assortment of complimentary parts, in accordance to the implementation produced in this project. The system developed to complete that task utilizes two PID controllers, one for controlling the throttle and the other to control the WR's heading. In order to achieve optimal system performance, it is important that the controller for steering includes throttle input into the equation, providing the solution with the capability to better handle varying velocities.

A navigation algorithm was also required in order to provide the PID controllers with functional reference values. A path based algorithm based upon a look ahead principle was able to fulfill this requirement, providing the controllers with the needed values. The algorithm was possible to adjust as desired by changing the distance of how far ahead the system is to look, in order to achieve different levels of regression regarding turn.

The project, however, was not able to prove that the solution is fully functional in a real life application due to delays in software development and a number of other factors, such as limited accessibility of trial opportunities with a functional actuator system. The final field tests are to be conducted after the report deadline.

## References

- [1] Sjörräddningssällskapet, “Om oss,” (visited 2019-02-05). [Online]. Available: <https://www.sjoraddning.se/om-oss>
- [2] D. of Electrical Engineering, “Autonomous WaveRunner - Follow the Leader,” (visited 2019-02-11). [Online]. Available: <https://www.chalmers.se/SiteCollectionDocuments/E2/Kandidatprojekt/2019/Automation/EENX15-19-02.pdf>
- [3] J. Manley, “Development of the autonomous surface craft “ACES”,” *Oceans Conference Record (IEEE)*, vol. 2, pp. 827 – 832 vol.2, 11 1997. [Online]. Available: <https://doi.org/10.1109/OCEANS.1997.624102>
- [4] J. E. Manley, A. Marsh, W. Cornforth, and C. Wiseman, “Evolution of the autonomous surface craft autocat,” in *OCEANS 2000 MTS/IEEE Conference and Exhibition. Conference Proceedings (Cat. No.00CH37158)*, vol. 1, Sep. 2000, pp. 403–408 vol.1. [Online]. Available: <https://doi.org/10.1109/OCEANS.2000.881292>
- [5] M. Caccia, “Autonomous surface craft: prototypes and basic research issues,” in *2006 14th Mediterranean Conference on Control and Automation*, June 2006, pp. 1–6. [Online]. Available: <https://doi.org/10.1109/MED.2006.328786>
- [6] M. Caccia, M. Bibuli, R. Bono, and G. Bruzzone, “Basic navigation, guidance and control of an unmanned surface vehicle,” *Autonomous Robots*, vol. 25, no. 4, pp. 349–365, Nov 2008. [Online]. Available: <https://doi.org/10.1007/s10514-008-9100-0>
- [7] D. Bäck, M. Christensen, J. Hansson, A. Henriksson, O. R. Skjølingstad, and F. Ödeen, “Fjärrstyrning av rescuerunner,” Göteborg, Sverige, 2018, bachelor’s thesis, Departement of Signals and Systems, Chalmers University of Technology. [Online]. Available: <http://publications.lib.chalmers.se/records/fulltext/255851/255851.pdf>
- [8] B. Hallhagen and E. Persson, “Adapting a small watercraft to autonomously follow a lead boat,” Master’s thesis, Departement of Signals and Systems, Chalmers University of Technology, 2016. [Online]. Available: <http://publications.lib.chalmers.se/records/fulltext/248966/248966.pdf>
- [9] A. Andersson, V. Bäckman, O. Grankvist, A. Sarvik, and O. Pantzare, “Autonom eskortering av rescuerunner,” Göteborg, Sverige, 2018, bachelor’s thesis, Departement of Signals and Systems, Chalmers University of Technology. [Online]. Available: <http://publications.lib.chalmers.se/records/fulltext/219294/219294.pdf>
- [10] A. Bergholtz and C.-A. Hernvall, “Waypoint-based path following system for a jet ski,” 2015. [Online]. Available: <http://publications.lib.chalmers.se/records/fulltext/218514/218514.pdf>
- [11] *Ellipse Product sheet*, SBG Systems, 2019. [Online]. Available: [https://www.sbg-systems.com/wp-content/uploads/Ellipse\\_Series\\_Leaflet.pdf](https://www.sbg-systems.com/wp-content/uploads/Ellipse_Series_Leaflet.pdf)
- [12] P. M. V. John P. Snyder, “An album of map projections,” 1989. [Online]. Available: <https://pubs.usgs.gov/pp/1453/report.pdf>
- [13] PROJ contributors, *PROJ coordinate transformation software library*, Open Source Geospatial Foundation, visited (2019-04-24). [Online]. Available: <https://proj4.org/>

- [14] B. Lennartson, *Reglerteknikens grunder*. Lund: Studentlitteratur AB, 2002.
- [15] C. W. Reynolds, “Steering behaviors for autonomous characters,” 1999. [Online]. Available: <https://citeseerx.ist.psu.edu/viewdoc/download?doi=10.1.1.16.8035&rep=rep1&type=pdf>
- [16] T. I. Fossen, *Handbook of marine craft hydrodynamics and motion control [electronic resource] = Vademecum de navium motu contra aquas et de motu gubernando*. Chichester, West Sussex : Wiley, 2011., 2011. [Online]. Available: <https://doi.org/10.1002/9781119994138>
- [17] K. Benedict and M. Kirchhoff, “Explaining ships dynamic and handling using matlab & simulink as simulation tool in teaching maritime students.” 2007. [Online]. Available: <https://csum-dspace.calstate.edu/bitstream/handle/10211.3/73264/Benedict%20-%20Explaining%20Ships%20Dynamic%20and%20Handling.pdf>
- [18] Engineering ToolBox, “Jet discharge propulsion,” 2013. [Online]. Available: [https://www.engineeringtoolbox.com/jet-discharge-propulsion-force-d\\_1868.html](https://www.engineeringtoolbox.com/jet-discharge-propulsion-force-d_1868.html)
- [19] M. V. Kothare, P. J. Campo, M. Morari, and C. N. Nett, “A unified framework for the study of anti-windup designs,” *Automatica*, vol. 30, no. 12, pp. 1869 – 1883, 1994. [Online]. Available: [https://doi.org/10.1016/0005-1098\(94\)90048-5](https://doi.org/10.1016/0005-1098(94)90048-5)
- [20] G. Guennebaud, B. Jacob *et al.*, “Eigen v3,” 2010. [Online]. Available: <http://eigen.tuxfamily.org>
- [21] overlord1123, “Lowpassfilter,” <https://github.com/overlord1123/LowPassFilter>, 2018.
- [22] J. H. Cheon, K. Han, S.-M. Hong, H. J. Kim, J. Kim, S. Kim, H. Seo, H. Shim, and Y. Song, “Toward a secure drone system: Flying with real-time homomorphic authenticated encryption,” *IEEE Access*, vol. 6, pp. 24 325 – 24 339, 2018. [Online]. Available: <http://dx.doi.org/10.1109/ACCESS.2018.2819189>

## A Git Repository Structure

Throughout the project a Git repository was used for version control. To ease the usage of the repository, an overview of the structure is provided; more detailed guidance is provided in the `README.md` files located inside the repository. The directory structure outlined here is accurate as per commit `ba98df0f2517dae04d4667c94637818f62ef54c0`.

The repository is publicly available at <https://github.com/autonomous-waverunner/follow-the-leader>.

